Working Paper Research

February 2024 No 446

Macroeconomic drivers of inflation expectations and inflation risk premia

by Jef Boeckx, Leonardo Iania and Joris Wauters

National Bank OF BELGIUM
Eurosystem

Publisher

Pierre Wunsch, Governor of the National Bank of Belgium

Statement of purpose

The purpose of these Working Papers is to promote the circulation of research results (Research Series) and analytical studies (Documents Series) made within the National Bank of Belgium or presented by external economists in seminars, conferences and conventions organised by the Bank. The aim is therefore to provide a platform for discussion. The opinions expressed are strictly those of the authors and do not necessarily reflect the views of the National Bank of Belgium.

The Working Papers are available on the website of the Bank: http://www.nbb.be

ISSN: 1375-680X (print)
ISSN: 1784-2476 (online)

Abstract

We propose a new model to decompose inflation swaps into genuine inflation expectations and risk premiums. We develop a no-arbitrage term structure model with stochastic endpoints, separating macroeconomic variables into transitory parts and long-run, economically grounded determinants, such as the equilibrium real interest rate and the inflation target. Our estimations deliver new insights into how macroeconomic variables affect market-based inflation expectation measures.

Keywords: Inflation-linked swaps, affine term structure model, inflation expectations, inflation risk premia, inflation trend, shifting endpoints.

JEL Codes: E31, E44, E52.

Authors:
Jef Boeckx, Economics and Research Department, National Bank of Belgium
- e-mail: Jef.Boeckx@nbb.be
Leonardo Iania, Université catholique de Louvain, LFIN/CORE
- e-mail: leonardo.iania@uclouvain.be
Joris Wauters, Economics and Research Department, National Bank of Belgium
- e-mail: Joris.Wauters@nbb.be

We thank Bruno De Backer, Marco Lyrio, our discussant Sarah Mouabbi, Alberto Plazzi, the participants to the 11th Bundesbank workshop on term structure modeling, and the seminars at the University of Calabria, the Banca d'Italia, and the European Central Bank for useful comments. The views expressed in this paper are solely those of the authors and not those of the National Bank of Belgium. All remaining errors are our responsibility. Leonardo Iania acknowledges the support of the following research grant: ARC 18/23-089.

Non-technical summary

Central banks in advanced economies aim to keep inflation stable around their inflation targets. The ECB, for instance, has a medium-term inflation target of 2%. When deciding on how to change their monetary policy instruments, central banks pay a great deal of attention to analyzing the behavior of inflation expectations, as they are an important determinant of the inflation outlook. When households, firms or financial markets expect future inflation to not be in line with the central bank's target, risks are large that inflation will indeed not stabilize around the central bank's aim. This paper offers a tool to assess how financial markets view future inflation and helps policymakers understand what factors are driving the market for inflation protection.

While inflation expectations are key to assessing the outlook for price stability, monitoring them in detail is challenging. Surveys conducted with households, firms or professional economists are one source of inflation expectations. Unfortunately, they are conducted only on an infrequent basis and may give conflicting signals regarding the private sector's inflation expectations. Financial markets offer another source of information on inflation expectations: inflation-linked swaps, whose returns are directly linked to the level of inflation and available for a wide range of maturities, have become an increasingly liquid asset class. Their availability at a very high frequency and the fact that traders have "skin in the game" when trading inflation products are obvious advantages of this information source. However, market participants also require compensation for the uncertain returns of investing in these products. That means their prices also contain risk premia and not only "pure" expectations of future inflation.

We propose a method to separate risk premia from "pure" expectations in the observed inflation-linked swap rates. We are not the first to do so, but the novelty of our approach consists in allowing for time-variation in trend inflation and the equilibrium real interest rate. The pronounced low-frequency movements in both variables motivate this feature, as one otherwise risks overestimating the importance of risk premia. The model also incorporates macroeconomic data, helping to provide intuition on what economic variables and shocks drive the pricing on inflation markets.

We estimate the model for the euro area and the US using data from January 2005 until August 2023, thus including the recent inflation spike. Several insights emerge. First, inflation risk premia are important drivers of inflation-linked swap rates – especially in the euro area during the period of low inflation. As of August 2023, the expectations component in 10-year inflation swaps stood at 1.99% and 1.94% for the euro area and the US, respectively. Second, including macroeconomic data in the model delivers more plausible longer-run behavior of the model as it avoids – unwarranted and unjustified – oscillating behavior of the deterministic part of the model. Third, macroeconomic factors are a primary source of variation in inflation-linked swaps, including in periods of large movements like during the Great Financial Crisis and the aftermath of the pandemic.

TABLE OF CONTENTS

1 Introduction

Achieving price stability is at the core of major central banks' mandates. Historically, after the oil crises of the 70s, the world's leading central banks have contributed to a general decrease and subsequent stability in inflation rates, which averaged around 2% in OECD economies in the 2010s. However, inflation rates have surged since mid-2021 to multi-decade highs. In such an uncertain environment, gauging information about inflation expectations is key for central bankers, policymakers, and investors. For example, inflation-targeting central banks aim to monitor whether inflation expectations are anchored to the inflation target.

Unfortunately, measuring inflation expectations is not an easy task. Approximate measures can be derived indirectly from financial markets (market-based measures) and by surveying consumers and professional forecasters (survey-based measures). Both measures have pros and cons. Survey-based measures of expected inflation give an idea of respondents' views about the inflation outlook. However, they are not timely, as they are only available at low frequencies and, to a certain extent, not easy to interpret and work with, as there is a great deal of heterogeneity among the different survey providers. Market-based measures of inflation expectations are extracted from financial contracts offering inflation hedges to market participants. They provide a timely and high-frequency measure of inflation expectations. Since market activities and actual trading determine them, they reflect the market's revealed – and not the stated – concerns about future inflation. However, the inflation measures obtained from those contracts are inaccurate because they contain a risk premium, compensating investors for the uncertain returns in such contracts.

This paper proposes a model that decomposes financial measures of inflation expectations into genuine inflation expectations and risk premia. The topic has attracted a considerable part of the macro-finance literature. Ang et al. (2008) develop a regime-switching Affine Term Structure Model (ATSM) with time-varying prices of risk and inflation to identify the relative contributions of real interest rates, expected inflation, and the inflation risk premium to changes in US nominal interest rates. Haubrich et al. (2012) estimate a model of nominal and real bond yield curves using data on Inflation-Linked Swap (ILS) rates, nominal Treasury yields, and inflation surveys. Christensen et al. (2010) and Joyce et al. (2010) build a standard affine model to jointly price nominal and real yields for the United States (US) and the United Kingdom (UK) and to study the evolution of the expected inflation and the inflation risk premium. Abrahams et al. (2016) extend the previous modeling framework to account for liquidity risk premia in inflation-linked government bonds. Carriero et al. (2018) introduce a shadow-rate term structure model for UK nominal and real yields to assess the impact of the recent Zero Lower-Bound (ZLB) period on inflation expectations and inflation risk premia. Hördahl and Tristani (2014) jointly model macroeconomic and term structure dynamics to estimate inflation risk premia and inflation expectations in the US and the Euro Area (EA). They consider data until 2014, hence excluding the recent low inflation period. More recently, Camba-Mendez and Werner (2017) developed model-free and model-based indicators for the inflation risk premium in the US and the EA using ILS data.

While this flourishing literature highlights the substantial effort devoted to disentangling inflation expectations from risk premia using market-based measures, some modeling and empirical questions remain open. For example: (i) What is the importance of long-term trend versus short-term macroeconomic dynamics in market-based measures

of inflation expectations (and inflation risk premia)? (ii) What is the impact of international factors? And finally, (iii) Are the long-term and short-term determinants of EA and US inflation risk premia and expectations similar?

To answer these questions, we build a novel ATSM with a stationary part of latent and macro variables and a random-walk block composed of long-run stochastic trends for trend inflation and the equilibrium real rate. As in the Joslin et al. (2011) setting, under the risk-neutral measure, ILS rates follow a low-dimensional factor structure with spanned factors, while the historical evolution of ILS rates, latent factors, macroeconomic variables, and stochastic trends is characterized by a higher-order vector error correction model, with theory-grounded cointegration relationships. The model builds on the works of Dewachter and Iania (2011), who propose a Macro-Finance model of the US nominal yield curve including macroeconomic, liquidity-related, and return forecasting factors, and of Bauer and Rudebusch (2020), who extend the normalization setting of Joslin et al. (2011) to account for stochastic trends. Hence, our modeling framework allows us to express ILS rates and the inflation risk premium as a function of (i) latent variables, namely the principal components of the ILS term structure; (ii) local macroeconomic variables, proxying for the target policy rate, inflation, and real activity; (iii) international trends on energy (oil) prices and commodity demand; and (iv) stochastic trends, linked to long-term inflation expectations and the natural real rate. We estimate the model on monthly US and EA data, using a state-space setting whereby we exploit several mixed-frequency sources of information to identify the stochastic trends, such as the quarterly survey data from the Surveys of Professional Forecasters and the monthly/bi-monthly and quarterly data from the Consensus Economics surveys. To ease the estimation burden and the over-fitting problem linked to parameter proliferation associated with the model's lag structure, we propose a penalized likelihood approach that shrinks high-order lag parameters (see Tibshirani, 1996; Fan and Li, 2001, among others, for early applications of this approach).

Our model delivers two main original results. First, the decomposition of ILS rates in an expected component (EC) and an inflation risk premium underscores that the latter is an important driver of ILS rates' variation, especially for the EA during the lowflation period. Furthermore, by further decomposing these two components in a deterministic and stochastic part (see Giannone et al., 2019), we point out that the EA latent factor models generate an oscillating behavior in the deterministic part of the EC. This problematic feature is absent in our model.

Second, we use our framework to extract the expected and the inflation risk premium component of ILS rates – labeled EC and IRP, respectively – and show how they relate to unspanned factor innovations. Unlike spanned factor innovations, these shocks can jointly affect yield curve principal components and macroeconomic variables on impact. The variance decompositions highlight that unspanned factor innovations are the main drivers of low-frequency movements of ILS rates. However, spanned factor shocks are a key component of the IRP variations, accounting for roughly one-fifth (half) of the US (EA) high- and low-frequency IRP movements. The historical decomposition highlights that unspanned factors are a primary source of ILS, EC, and IRPs' variation around key historical episodes such as the Great Financial Crisis (GFC) and the 2010s oil price glut.

In the rest of the paper, we outline our model in Section 2, present the dataset and the estimation strategy in Section 3, report and discuss our results in Section 4, and finally, we draw the concluding remarks in Section 5. Appendix A reports additional results and parameter estimates.

2 Modeling approach

2.1 Term structure modeling

Defining the Inflation-Linked Swap (ILS) contracts.
A zero-coupon ILS is a contract by which, at maturity, the floating leg counterpart receives a payment linked to the realized inflation rate throughout the contract (n), $\pi_{t+n,t} = \frac{P_{t+n}}{P_t} - 1$. In exchange, this party pays an amount linked to a fixed rate, $Y_{n,t}$, established at the initiation of the contract.[1] Since there is no exchange of money at the initiation of the contract, the expected value of the two payments should be equal:

$$\underbrace{\mathbb{E}_t^p\Big[M_{t,t+n}\big[(1+Y_{n,t})^n - 1\big]\Big]}_{\text{Fixed leg}} = \underbrace{\mathbb{E}_t^p\big[M_{t,t+n}\pi_{t+n,t}\big]}_{\text{Floating leg}} \quad p = \mathbb{P}, \mathbb{Q}, \tag{1}$$

where $M_{t,t+n}$ is the stochastic discount factor. The equality reported in equation (1) is valid in probability settings adjusted for risk, namely risk-neutral probability measures $\mathbb{Q}$, or not, i.e., the historical probability measures $\mathbb{P}$. As shown by Camba-Mendez and Werner (2017), pricing the contract under the risk-neutral measure simplifies equation (1) as:

$$y_{n,t} = \frac{1}{n} log(\mathbb{E}_t^{\mathbb{Q}} e^{\sum_{j=1}^{n} \pi_{t+j}}), \tag{2}$$

where $y_{n,t}$ is the continuous time counterpart of $Y_{n,t}$ and π_{t+j} is the inflation rate between two consecutive periods, *t+j-1* and *t+j*. Equation (2) highlights that, in the risk-neutral probabilistic setting, the (continuously compounded) ILS rate is the expected average one-period inflation rate throughout the contract.

Accounting for risk.
We analyze the risk compensation in ILS contracts by focusing on the inflation risk premium and the forward risk premium obtained via the decomposition of ILS and forward rates in expected and risk premium components, respectively. We use our dynamic term structure modeling setting to decompose $y_{n,t}$ in EC and IRP components:

$$y_{n,t} = y_{n,t}^{EC} + y_{n,t}^{IRP}, \tag{3}$$

where $y_{n,t}^{EC}$ is the average expected inflation free of the inflation risk premium, and $y_{n,t}^{IRP}$ represents the compensation required by market participants for their exposure to the model's risk factors. We obtain the decomposition in equation (3) in two steps. First, following Camba-Mendez and Werner (2017), we employ a Gaussian affine no-arbitrage setting to price the ILS contracts. ILS rates are expressed as an affine function of the risk factors $\mathcal{Z}_t$, identified in Section 2.2, by setting (i) the one-period ILS rate, $y_{1,t}$, an affine function of $\mathcal{Z}_t$, and (ii) by assuming that the risk factors have affine Gaussian dynamics under both probability measures:

$$y_{1,t} = \rho_0 + \boldsymbol{\rho}_1' \mathcal{Z}_t \tag{4a}$$

$$\mathcal{Z}_t = \boldsymbol{\mu}^i + \boldsymbol{\Phi}^i \, \mathcal{Z}_{t-1} + \boldsymbol{\Sigma}\boldsymbol{\varepsilon}_t^i, \quad \boldsymbol{\varepsilon}_t^i \sim \mathcal{N}(\mathbf{0}, \boldsymbol{I}) \text{ and } i = \mathbb{Q}, \mathbb{P}, \tag{4b}$$

[1] The exchange of payments is performed at maturity, and the exact quantity of cash to exchange is proportional to the contract's notional amount, multiplied by the realized inflation rate and the swap rate.

where $\rho_0, \boldsymbol{\rho}_1, \boldsymbol{\mu}^{\mathbb{P}}, \boldsymbol{\mu}^{\mathbb{Q}}, \boldsymbol{\Phi}^{\mathbb{P}}, \boldsymbol{\Phi}^{\mathbb{Q}}$, and $\boldsymbol{\Sigma}$ are (potential) model parameters while $\boldsymbol{I}$ is an identity matrix of conformable dimension. The parameters of equation (4b) under $\mathbb{Q}$ determine the pricing of the cross-sections of ILS rates, while the $\mathbb{P}$ parameters are key for the risk/term premium evolution. In our setting, the link between the two measures is obtained by assuming (i) essentially affine market prices of risk, $\boldsymbol{\Lambda}_t$, and (ii) a stochastic discount factor exponentially affine on the short-term ILS rate and $\boldsymbol{\Lambda}_t$:

$$\boldsymbol{\Lambda}_t = \boldsymbol{\Sigma}^{-1}\left(\boldsymbol{\lambda}_0 + \boldsymbol{\lambda}_1 \mathcal{Z}_t\right), \quad \boldsymbol{\mu}^{\mathbb{Q}} = \boldsymbol{\mu}^{\mathbb{P}} - \boldsymbol{\lambda}_0, \quad \boldsymbol{\Phi}^{\mathbb{Q}} = \boldsymbol{\Phi}^{\mathbb{P}} - \boldsymbol{\lambda}_1 \tag{5a}$$

$$M_{t,t+1} = \exp(-y_{1,t} - \frac{1}{2}\boldsymbol{\Lambda}_t'\boldsymbol{\Lambda}_t - \boldsymbol{\Lambda}_t'\boldsymbol{\Sigma}\boldsymbol{\varepsilon}_t^{\mathbb{P}}). \tag{5b}$$

Under these assumptions, it is possible to express $y_{n,t}$ as an affine function of the risk factors, $\mathcal{Z}_t$:

$$y_{n,t} = a_n + \boldsymbol{b}_n \mathcal{Z}_t, \tag{6}$$

whereby the weights of (6) derive from the standard Riccati equations (see Ang and Piazzesi, 2003). Specifically, $a_n = -n^{-1}a_n$ and $\boldsymbol{b}_n = -n^{-1}b_n$

$$a_n = a_{n-1} + b_{n-1}\boldsymbol{\mu}^{\mathbb{Q}} + \frac{1}{2}b_{n-1}\boldsymbol{\Sigma}\boldsymbol{\Sigma}'b_{n-1} - \rho_0 \tag{7a}$$

$$b_n = \boldsymbol{\Phi}^{\mathbb{Q}'}b_{n-1} - \boldsymbol{\rho}_1. \tag{7b}$$

Second, to obtain an expression for the EC of $y_{n,t}$, i.e., the part of the ILS rates net from the risk compensations, we first switch off risk compensation by setting $\boldsymbol{\lambda}_0$ and $\boldsymbol{\lambda}_1$ to zero in equation (5a). Subsequently, we derive a new set of loadings, a_n^{EC} and $\boldsymbol{b}_n^{EC}$, by iterating the Riccati equations with $\boldsymbol{\mu}^{\mathbb{P}}$ and $\boldsymbol{\Phi}^{\mathbb{P}}$ instead of $\boldsymbol{\mu}^{\mathbb{Q}}$ and $\boldsymbol{\Phi}^{\mathbb{Q}}$. As a result, the EC of $y_{n,t}$ is:

$$y_{n,t}^{EC} = a_n^{EC} + \boldsymbol{b}_n^{EC}\mathcal{Z}_t, \tag{8}$$

and the loadings for the inflation risk premium (IRP) component of $y_{n,t}$ are obtained from equation (3) and equations (8) and (6):

$$y_{n,t}^{IRP} = y_{n,t} - y_{n,t}^{EC} \tag{9a}$$

$$= a_n - a_n^{EC} + (\boldsymbol{b}_n - \boldsymbol{b}_n^{EC})\mathcal{Z}_t \tag{9b}$$

$$= a_n^{IRP} + \boldsymbol{b}_n^{IRP}\mathcal{Z}_t. \tag{9c}$$

In other words, the IRP is the difference between the fitted inflation swaps and the expected inflation rate (EC). It will be positive (negative) when the inflation swaps are above (below) the expected inflation rate.

2.2 Dynamic system

Risk factors.
Our set of risk factors includes (up to) ten variables, divided in four categories: (i) two global variables $\mathbf{w}_t = [g_t^w, p_t^o]'$, proxying for global real economic activity (percent deviations from trend), and the log of real oil prices, respectively; (ii) three country-specific macro variables $\mathbf{m}_t = [\pi_t, g_t, i_t]'$, proxying for inflation, π_t, economic activity, g_t, and the policy rate, i_t; (iii) three ILS principal components,[2] the level, l_t, the slope, s_t,

[2]In Section 3.1.1 we report the loadings of the three principal components and show that they can be interpreted as level, slope, and curvature.

and the curvature, c_t, all stacked in $\mathbf{p}_t = [l_t, s_t, c_t]'$ and equal to $\mathbf{p}_t = W_p Y_t$, and (iv) two stochastic trends, one for inflation, π_t^*, and another for the equilibrium real rate, r_t^*, collected in the vector $\boldsymbol{\xi}_t = [\pi_t^*, r_t^*]'$.

The motivation for selecting the two international variables builds on several recent studies and policy notes investigating the interplay between oil prices and inflation expectations in the US and the EA, even if we refrain from building a model with structural identification of the oil shocks. For the US, the two recent studies by Aastveit et al. (2023) and Kilian and Zhou (2022) use a structural model to assess how oil (or gasoline) shocks affect US consumer inflation expectations. They both conclude that oil shocks impact short-term inflation expectations. For the EA, the Eurosystem's Expert Group on Inflation Expectations dedicated a section of their report to investigating the link between inflation expectations and oil prices in the EA. Using structural identification for oil shocks, they conclude that only short-term expectations react to global real activity and oil-specific demand shocks (see Baumann et al., 2021).[3]

Local macroeconomic variables (or news related to them) have been found to affect market-based inflation expectations. For example, Galati et al. (2011) show that ILS-based indicators of inflation expectations became more sensitive to news about inflation and other domestic macroeconomic variables. Finally, the two stochastic trends work as the long-term time-varying expected value of inflation, the ILS PCs (the stochastic trend for inflation), and the short-term interest rates (the stochastic trend for the real rate). We provide additional motivation for our selected variables in the appendix, Section A.2.

The time series evolution[4] of the global factors, the country-specific variables, and the principal components are summarized via a vector error-correction setting:

$$\begin{bmatrix} \mathbf{w}_t \\ \mathbf{m}_t \\ \mathbf{p}_t \end{bmatrix} = \underbrace{\sum_{\upsilon=1}^{\Upsilon} \begin{bmatrix} \boldsymbol{\Phi}_\upsilon^w & \mathbf{0} & \mathbf{0} \\ \boldsymbol{\Phi}_\upsilon^{mw} & \boldsymbol{\Phi}_\upsilon^m & \mathbf{0} \\ \boldsymbol{\Phi}_\upsilon^{pw} & \boldsymbol{\Phi}_\upsilon^{pm} & \boldsymbol{\Phi}_\upsilon^p \end{bmatrix} \begin{bmatrix} \mathbf{w}_{t-\upsilon} - \boldsymbol{\mu}^w - \boldsymbol{\Gamma}^w \boldsymbol{\xi}_t \\ \mathbf{m}_{t-\upsilon} - \boldsymbol{\mu}^m - \boldsymbol{\Gamma}^m \boldsymbol{\xi}_t \\ \mathbf{p}_{t-\upsilon} - \boldsymbol{\mu}^p - \boldsymbol{\Gamma}^p \boldsymbol{\xi}_t \end{bmatrix}}_{\text{Short-term component}} + \underbrace{\begin{bmatrix} \boldsymbol{\mu}^w \\ \boldsymbol{\mu}^m \\ \boldsymbol{\mu}^p \end{bmatrix} + \begin{bmatrix} \boldsymbol{\Gamma}^w \\ \boldsymbol{\Gamma}^m \\ \boldsymbol{\Gamma}^p \end{bmatrix} \boldsymbol{\xi}_t}_{\text{Long-term component}} + \underbrace{\begin{bmatrix} \boldsymbol{\Sigma}^w & \mathbf{0} & \mathbf{0} \\ \boldsymbol{\Sigma}^{mw} & \boldsymbol{\Sigma}^m & \mathbf{0} \\ \boldsymbol{\Sigma}^{pw} & \boldsymbol{\Sigma}^{pk} & \boldsymbol{\Sigma}^p \end{bmatrix} \begin{bmatrix} \boldsymbol{\varepsilon}_t^w \\ \boldsymbol{\varepsilon}_t^m \\ \boldsymbol{\varepsilon}_t^p \end{bmatrix}}_{\text{Innovations}}, \qquad \begin{bmatrix} \boldsymbol{\varepsilon}_t^w \\ \boldsymbol{\varepsilon}_t^m \\ \boldsymbol{\varepsilon}_t^p \end{bmatrix} \sim \mathcal{N}(\mathbf{0}, \boldsymbol{I}), \quad (10)$$

where $\boldsymbol{I}$ is an identity matrix of conformable dimension. Equation (10) is the multivariate and multi-lag extension of Kozicki and Tinsley (2001) and Dewachter and Iania (2011).

Short-term dynamics.
The short-term component of equation (10) describes how innovations to the system – brought about by the three sets of normally distributed shocks $\boldsymbol{\varepsilon}_t^w$, $\boldsymbol{\varepsilon}_t^m$, and $\boldsymbol{\varepsilon}_t^p$ – propagate through time, causing a deviation of $\mathbf{w}_t$, $\mathbf{m}_t$, and $\mathbf{p}_t$ from their long-run values. Under suitable stability conditions, see infra, if no additional shocks hit the system, these deviations converge to zero.

[3] Among other, Galati et al. (2018) reaches a similar conclusion about the relationship between oil prices and short-term inflation expectations, but without using any structural identification of the oil market's shocks.

[4] Note that the probability measure of reference is the historical one, but, to ease notation, we drop the superscript $\mathbb{P}$.

Three points are worth mentioning regarding the parameters included in the short-term and innovations components. First, $\mathbf{\Sigma}^w$,$\mathbf{\Sigma}^m$, and $\mathbf{\Sigma}^p$ are lower triangular, reflecting a Cholesky ordering of the shocks, with international factors being the most exogenous, followed by the country-specific factors and the principal components. For the international factors, the most exogenous innovation is real economic activity, while the ordering of country-specific factors follows the literature in assuming that supply shocks are the most exogenous, followed by demand shocks. Second, we impose that the ILS factors do not affect the evolution of the macro variables and that local macro variables do not affect the evolution of the international factors. This restriction is guaranteed by the Cholesky ordering and by imposing that $\mathbf{\Phi}_{\upsilon}^{wm}, \mathbf{\Phi}_{\upsilon}^{wp}, \mathbf{\Phi}_{\upsilon}^{mp} = \mathbf{0}\ \forall \upsilon$.[5] Third, following Joslin et al. (2013), we select a parsimonious one-lag structure on the ILS principal components by imposing that $\mathbf{\Phi}_{\upsilon}^{p} = \mathbf{0}\ \forall \upsilon > 1$.

Long-run dynamics.
To analyze the long-run behavior of $\mathbf{w}_t$, $\mathbf{m}_t$, and $\mathbf{p}_t$, we specify a random walk process for the stochastic trends, and we conveniently write equation (10) in more compact form by defining $\mathbf{x}_t = [\mathbf{w}_t', \mathbf{m}_t', \mathbf{p}_t']'$:

$$\mathbf{x}_t = \sum_{\upsilon=1}^{\Upsilon} \mathbf{\Phi}_{\upsilon}^{x}(\mathbf{x}_{t-\upsilon} - \boldsymbol{\mu}^x - \mathbf{\Gamma}^x \boldsymbol{\xi}_t) + \boldsymbol{\mu}^x + \mathbf{\Gamma}^x \boldsymbol{\xi}_t + \mathbf{\Sigma}^x \boldsymbol{\varepsilon}_t^x, \quad \boldsymbol{\varepsilon}_t^x \sim \mathcal{N}(\mathbf{0}, \boldsymbol{I}) \tag{11a}$$

$$\boldsymbol{\xi}_t = \boldsymbol{\xi}_{t-1} + \mathbf{\Sigma}^{\xi} \boldsymbol{\eta}_t, \quad \boldsymbol{\eta}_t \sim \mathcal{N}(\mathbf{0}, \boldsymbol{I}), \tag{11b}$$

where superscript x denotes the compact vectors/matrices of equation (10). The long-run conditional expectation of $\mathbf{x}_{t+j}$, i.e. $\lim_{j\to\infty} \mathbb{E}^{\mathbb{P}}[\mathbf{x}_{t+j}|\mathcal{I}_t]$, relies on roots of the polynomial $\mathbf{\Phi}^x(\mathcal{L}) = \mathbf{\Phi}_1^x + \mathbf{\Phi}_2^x \mathcal{L} + ... + \mathbf{\Phi}_{\Upsilon-1}^x \mathcal{L}^{\Upsilon-1}$, defined in the lag operator $\mathcal{L}\mathbf{x}_t = \mathbf{x}_{t-1}$. If all roots of $I - \mathbf{\Phi}^x(\mathcal{L})$ lie outside the unit circle, the short-term component of equation (11a) (or equivalently equation (10)) shrinks to zero. As a consequence:

$$\lim_{j\to\infty} \mathbb{E}[\mathbf{x}_{t+j}|\mathcal{I}_t] = \boldsymbol{\mu}^x + \mathbf{\Gamma}^x \boldsymbol{\xi}_t, \tag{12}$$

which implies that the long-run expectations of the macro variables and the principal components incorporate a constant and a stochastic part, equal to $\mathbf{\Gamma}^x \boldsymbol{\xi}_t$ and governed by the cointegration matrices $\mathbf{\Gamma}^x = [\mathbf{\Gamma}^{w'}, \mathbf{\Gamma}^{m'}, \mathbf{\Gamma}^{p'}]'$, see equation (10), and the evolution of the stochastic trends $\boldsymbol{\xi}_t$, see equation (11b). Our three sets of assumptions for the long-run components of $\mathbf{x}_t$ are summarized below:

$$\boldsymbol{\mu}^{\mathbf{w}} = \begin{bmatrix} 0 \\ 0 \end{bmatrix}, \quad \boldsymbol{\mu}^{\mathbf{m}} = \begin{bmatrix} \mu^{\pi} \\ 0 \\ \mu^{i} \end{bmatrix}, \quad \boldsymbol{\mu}^{\mathbf{p}} = \begin{bmatrix} \mu^{l} \\ \mu^{s} \\ \mu^{c} \end{bmatrix}, \tag{13a}$$

$$\mathbf{\Gamma}^{\mathbf{w}} = \begin{bmatrix} 0 & 0 \\ 0 & 0 \end{bmatrix}, \quad \mathbf{\Gamma}^{\mathbf{m}} = \begin{bmatrix} 1 & 0 \\ 0 & 0 \\ 1 & 1 \end{bmatrix}, \quad \mathbf{\Gamma}^{\mathbf{p}} = \begin{bmatrix} \gamma^{l} & 0 \\ \gamma^{s} & 0 \\ \gamma^{c} & 0 \end{bmatrix}. \tag{13b}$$

First, we assume stationarity for the demeaned global economic factors, $\mathbf{\Gamma}^{\mathbf{w}} = \mathbf{0}$ and $\boldsymbol{\mu}^{\mathbf{w}} = \mathbf{0}$. Second, for the local economic factors, we assume that the Fisher (1896)

[5] The results are equivalent when we relax the condition that $\mathbf{\Phi}_{\upsilon}^{wm} = \mathbf{0}$.

equation holds in the long run, and we demeaned the measure of real activity, $\boldsymbol{\mu}^{\mathbf{m}} = \mathbf{0}$, implying:

$$\lim_{j\to\infty} \mathbb{E}[\pi_{t+j}|\mathcal{I}_t] = \pi_t^* \tag{14a}$$

$$\lim_{j\to\infty} \mathbb{E}[g_{t+j}|\mathcal{I}_t] = 0 \tag{14b}$$

$$\lim_{j\to\infty} \mathbb{E}[i_{t+j}|\mathcal{I}_t] = \pi_t^* + r_t^*. \tag{14c}$$

Finally, to derive the long-term relationships for the ILS factors, we start from the intuition that, under the historical probability measure, for any maturity, the long-run expected value of the ILS rates converges to

$$\lim_{j\to\infty} \mathbb{E}[y_{n,t+j}|\mathcal{I}_t] = \psi_n + \pi_t^*, \tag{15}$$

where ψ_n is a maturity-dependent constant accounting for potential premiums linked, for example, to liquidity. Next, since l_t, s_t, and c_t are a linear combination of the N ILS rates, collected in $Y_t = [y_{1,t}, ..., y_{N,t}]'$, we obtain:

$$\lim_{j\to\infty} \mathbb{E}[l_{t+j}|\mathcal{I}_t] = w_l Y_t = w_l(\boldsymbol{\psi} + \boldsymbol{\iota}\pi_t^*) = w_l\boldsymbol{\psi} + w_l\boldsymbol{\iota}\pi_t^* \tag{16a}$$

$$\lim_{j\to\infty} \mathbb{E}[s_{t+j}|\mathcal{I}_t] = w_l Y_t = w_s(\boldsymbol{\psi} + \boldsymbol{\iota}\pi_t^*) = w_s\boldsymbol{\psi} + w_s\boldsymbol{\iota}\pi_t^* \tag{16b}$$

$$\lim_{j\to\infty} \mathbb{E}[c_{t+j}|\mathcal{I}_t] = w_c Y_t = w_c(\boldsymbol{\psi} + \boldsymbol{\iota}\pi_t^*) = w_c\boldsymbol{\psi} + w_c\boldsymbol{\iota}\pi_t^*, \tag{16c}$$

where $\boldsymbol{\iota}$ is an N-dimensional column vector of ones and $\boldsymbol{\psi}$ is defined as $\boldsymbol{\psi} = [\psi_1, \psi_2, ..., \psi_N]'$. The long-run relationships expressed in equations (16a) to (16c) have the following implication for $\boldsymbol{\mu}^{\mathbf{P}}$ and $\boldsymbol{\Gamma}^{\mathbf{P}}$. First, the elements of $\boldsymbol{\Gamma}^{\mathbf{P}}$ governing the cointegration relationship between the stochastic trend of inflation and the ILS principal components (γ^l, γ^s, γ^c) are fixed to $w_l\boldsymbol{\iota}$, $w_s\boldsymbol{\iota}$, and $w_c\boldsymbol{\iota}$, respectively. Second, the constant parts of the long-term components of $\mathbf{p}_t$, i.e., the elements of $\boldsymbol{\mu}^{\mathbf{P}}$, are simply a linear combination of the individual ψ's, which we treat as unknown parameters.

By defining $\mathbf{x}_t^{1:\Upsilon} = [\mathbf{x}_t', ..., \mathbf{x}_{t-\Upsilon+1}']'$ and $\mathcal{Z}_t = [\mathbf{x}_t^{1:\Upsilon'}, \boldsymbol{\xi}_t']'$, and stacking the shocks in $\boldsymbol{\epsilon}_t^{\mathbb{P}} = [\boldsymbol{\varepsilon}_t^{x'}, \boldsymbol{\eta}_t']'$, we express the dynamic system in its companion form, which corresponds to equation (4b) under $\mathbb{P}$:

$$\mathcal{Z}_t = \boldsymbol{\mu}^{\mathbb{P}} + \boldsymbol{\Phi}^{\mathbb{P}}\mathcal{Z}_{t-1} + \boldsymbol{\Sigma}\boldsymbol{\epsilon}_t^{\mathbb{P}}, \quad \boldsymbol{\epsilon}_t^{\mathbb{P}} \sim \mathcal{N}(\mathbf{0}, \boldsymbol{I}). \tag{17}$$

The next section lays out the identification restrictions to equation (4b) under $\mathbb{Q}$.

2.3 Canonical representation

We adopt the normalization of Joslin et al. (2011), henceforth JSZ, and extend the setting of Bauer and Rudebusch (2020) to two stochastic trends, which we apply to the ILS market. The JSZ identification technique dramatically reduces the number of parameters of equation (4b) under $\mathbb{Q}$ via two sets of restrictions. First, it imposes the so-called spanning conditions, i.e., under $\mathbb{Q}$ only a few linear combinations of Y_t – $\mathbf{p}_t$ for our model – span the cross-section of ILS rates over time. Hence,

$$\mathbb{E}^{\mathbb{Q}}[y_{n,t+j}|\mathcal{Z}_t] = \mathbb{E}^{\mathbb{Q}}[y_{n,t+j}|\mathbf{p}_t]. \tag{18}$$

To satisfy condition (18), we impose that, in the risk-neutral dynamics, equations (4a) and (4b) depend only on $\mathbf{p}_t$:

$$y_{1,t} = \rho_0 + \boldsymbol{\rho}_1^{p'} \mathbf{p}_t \tag{19a}$$

$$\mathbf{p}_t = \boldsymbol{\mu}^{\mathbb{Q},p} + \boldsymbol{\Phi}^{\mathbb{Q},p}\, \mathbf{p}_{t-1} + \boldsymbol{\Sigma}^p \boldsymbol{\varepsilon}_t^{\mathbb{Q},p}, \quad \boldsymbol{\varepsilon}_t^{\mathbb{Q},p} \sim \mathcal{N}(\mathbf{0}, \boldsymbol{I}_{N_p}), \tag{19b}$$

where the 3×1 vectors $\boldsymbol{\rho}_1^{p'}$ and $\boldsymbol{\mu}^{\mathbb{Q},p}$ and the 3×3 matrices $\boldsymbol{\Phi}^{\mathbb{Q},p}$ and $\boldsymbol{\Sigma}^p$ are the non-zero components of $\boldsymbol{\rho}_1'$, $\boldsymbol{\mu}^{\mathbb{Q}}$, $\boldsymbol{\Phi}^{\mathbb{Q}}$, and $\boldsymbol{\Sigma}$ in equation (4b) corresponding to $\mathbf{p}_t$. $\boldsymbol{\Sigma}$ also appears in equation (10) as the change of measure does not affect the variance of the shocks. Equations (19a) and (19b) imply that the ILS rates are an affine function of $\mathbf{p}_t$. Hence, equation (6) simplifies to:

$$y_{n,t} = a_n^p + \boldsymbol{b}_n^p \mathbf{p}_t, \tag{20}$$

where the loadings are obtained similarly as in equations (7a) and (7b), namely, $a_n^p = -n^{-1} a_n^p$ and $\boldsymbol{b}_n^p = -n^{-1} b_n^p$ with:

$$a_n^p = a_{n-1}^p + b_{n-1}^p \boldsymbol{\mu}^{\mathbb{Q},p} + \frac{1}{2} b_{n-1}^p \boldsymbol{\Sigma}^{\boldsymbol{p}} (b_{n-1}^p \boldsymbol{\Sigma}^{\boldsymbol{p}})' - \rho_0 \tag{21a}$$

$$b_n^p = (\boldsymbol{\Phi}^{\mathbb{Q},p})' b_{n-1}^p - \boldsymbol{\rho}_1^p. \tag{21b}$$

Looking at equations (19a), (19b), and (20), we notice that the spanning condition (18) is trivially satisfied as ILS rates at any maturity depend only on $\mathbf{p}_t$, which in turn, under $\mathbb{Q}$ depends only on its lagged value. The spanning assumption imposes a set of zero restrictions on the stochastic discount factor and the prices of risks, see equations (5a) and (5b), implying that:

$$M_{t,t+1} = \exp(-y_{1,t} - \frac{1}{2} \boldsymbol{\Lambda}_t^{p'} \boldsymbol{\Lambda}_t^p - \boldsymbol{\Lambda}_t^{p'} \boldsymbol{\Sigma}^p \boldsymbol{\varepsilon}_t^{\mathbb{P},p}) \tag{22a}$$

$$\boldsymbol{\Lambda}_t^p = \boldsymbol{\Sigma}^{p^{-1}} \left(\boldsymbol{\lambda}_0^p + \boldsymbol{\lambda}_1^p \mathcal{Z}_t \right) \tag{22b}$$

$$\boldsymbol{\lambda}_0^p = \boldsymbol{D}_p \boldsymbol{\mu}^{\mathbb{P}} - \boldsymbol{\mu}^{\mathbb{Q},p} \tag{22c}$$

$$\boldsymbol{\lambda}_1^p = \boldsymbol{D}_p \boldsymbol{\Phi}^{\mathbb{P}} - [\mathcal{O}\ \boldsymbol{\Phi}^{\mathbb{Q},p}], \tag{22d}$$

with $\mathcal{O}$ a zero-entry matrix of conformable dimension and $\boldsymbol{D}_p = [\mathcal{O}\ \boldsymbol{I}_{3\times 3}]$ a matrix selecting the last three rows of $\boldsymbol{\mu}^{\mathbb{P}}$ and $\boldsymbol{\Phi}^{\mathbb{P}}$, i.e. the parts related to $\mathbf{p}_t$. In a nutshell, as the cross-section of ILS rates is summarized by $\mathbf{p}_t$, only shocks to those principal components are priced, see equation (22a). However, via equations (22a) and (22b), unspanned factors play a role in the pricing of those shocks, which are weighted by the 3×1 prices of risk vector $\boldsymbol{\Lambda}_t^p$, that in turn is linked to all the variables of the dynamic system (17) via the matrix $\boldsymbol{\lambda}_1^p$ of equation (22b).

To identify the risk-neutral parameters, we follow JSZ and impose a second set of restrictions identifying restrictions on the $\mathbb{Q}$-dynamics, so that the real-world dynamics can be estimated without restrictions. We start with $N = 3$ latent factors $\mathcal{X}_t$ and impose the following restrictions on their $\mathbb{Q}$-dynamics:

$$y_{1,t} = \iota \mathcal{X}_t, \quad \boldsymbol{\mu}^{\mathcal{X}} = \begin{bmatrix} \boldsymbol{\kappa}^{\mathcal{X}} \\ 0 \\ 0 \end{bmatrix}, \quad \boldsymbol{\Phi}^{\mathcal{X}} = \begin{bmatrix} \boldsymbol{\lambda}_1^{\mathcal{X}} & 0 & 0 \\ 0 & \boldsymbol{\lambda}_2^{\mathcal{X}} & 0 \\ 0 & 0 & \boldsymbol{\lambda}_3^{\mathcal{X}} \end{bmatrix}, \tag{23}$$

where ι is 1×3 vector of ones and the $\boldsymbol{\lambda}^{\mathcal{X}}$s are assumed to be less than one in absolute value. Subsequently, we obtain the term structure loadings related to $\mathcal{X}_t$, $A_{\mathcal{X}}$, and $B_{\mathcal{X}}$, and use the definition of $\mathbf{p}_t = W_p Y_t$ to obtain the loadings for $\mathbf{p}_t$ in function of the parameters in (23):

$$Y_t = (I - B_{\mathcal{X}}(W_p B_{\mathcal{X}})^{-1} W_p) A_{\mathcal{X}} + B_{\mathcal{X}}(W_p B_{\mathcal{X}})^{-1} \mathbf{p}_t, \tag{24}$$

where $A_{\mathcal{X}}$ and $B_{\mathcal{X}}$ are the affine yield loadings on $\mathcal{X}_t$ and $W_p = [w_l', \ w_s', \ w_c']'$.

3 Empirical implementation

3.1 Data and preliminary statistics

We estimate the model for the EA and the US using a mix of quarterly and monthly data from January 2005 to August 2023. Our empirical analysis combines four types of information: data on ILS rates, macroeconomic variables, survey forecasts, and model-based long-run trend estimates from the literature.

3.1.1 ILS data

The swap series are from Bloomberg. We construct a monthly series by taking the end-of-the-month data from the daily ILS rates with maturity 1 to 10, 12, 15, 20, 25, and 30 years, collected in the vector Y_t. Panel A (B) of Table 1 reports the summary statistics of the EA (US) 1-, 5-, 10-, and 30-year maturity ILS rates. In both regions, ILS rates are characterized by upward-sloping averages, decreasing volatility, short-term leptokurtosis (fat tails), and increasing persistence (EA 30-year rates are not more persistent than 10-year inflation swaps). US ILS rates are, on average, higher and less persistent than the EA counterparts. Short-term (long-term) US ILS rates[6] are 0.3 pp. (0.5 pp.) higher than the European ones: 1.7% vs. 1.4% (2.6% vs. 2.1%). Average US ILS rates are above the 2% target of the Federal Reserve. This difference might be due to the Federal Reserve's inflation target being based on the Personal Consumption Expenditure index, which delivers, on average, lower inflation rates than the Consumer Price Index, the underlying index in ILS contracts. Panels A and B of Figure 1 indicate that EA and US long-term ILS rates, i.e., above ten years of maturity, display a declining trend from around 2013 until September 2020. The recent COVID crisis and the Russian aggression against Ukraine reverted this trend, causing the longest observed inversion in the term structure of ILS rates in both regions.

[6]Short-term and long-term refer to 1-year and 30-year maturity, respectively.

Table 1: Summary statistics: ILS rates and PCs

(A) EA ILS

	μ	σ	s	k	ρ_1	ρ_3
1-year	0.017	0.013	1.961	8.902	0.945	0.839
5-year	0.017	0.006	0.018	2.499	0.960	0.879
10-year	0.018	0.005	-0.282	2.128	0.970	0.905
30-year	0.021	0.004	-0.540	2.428	0.966	0.885

(B) US ILS

μ	σ	s	k	ρ_1	ρ_3
0.018	0.012	-1.087	8.246	0.908	0.626
0.022	0.005	-0.661	4.661	0.919	0.665
0.024	0.004	-0.640	2.992	0.923	0.751
0.025	0.004	-0.241	2.300	0.936	0.822

(C) EA PCs

	μ	σ	s	k	ρ_1	ρ_3	$\frac{\lambda_j}{\sum\lambda_n}$
PC 1	0.063	0.024	0.493	3.530	0.960	0.871	0.898
PC 2	-0.028	0.008	0.899	4.719	0.948	0.864	0.094
PC 3	0.011	0.002	0.358	2.351	0.844	0.728	0.006

(D) US PCs

μ	σ	s	k	ρ_1	ρ_3	$\frac{\lambda_j}{\sum\lambda_n}$
0.075	0.021	-0.827	5.827	0.919	0.663	0.856
-0.048	0.008	0.132	2.138	0.930	0.858	0.132
-0.002	0.002	-0.566	6.618	0.638	0.259	0.007

Notes: Panel A (B) reports the summary statistics of the EA (US) ILS rates with maturities of 1, 5, 10, and 30 years. Panel C (D) reports the summary statistics of the EA (US) first three principal components (PCs) of all the ILS rates. Symbols: μ = average; σ = standard deviation; s = skewness; k = kurtosis; ρ_1 = first order autocorrelation; ρ_3 = third order autocorrelation; λ_j = eigenvalue associated with the j-*th* principal component.

From vector Y_t, we extract for each country the first three principal components $PC1_t$, $PC2_t$, and $PC3_t$, whose statistics, plots and loadings are reported in panels C and D of Table 1, in panels C to F of Figure 1, respectively. Notably, in both regions, the first three principal components capture more than 99% of the total variation, with the first factor responsible for about 90% of the variation in the EA and 86% for the US.

Figure 1: ILS rates, principal components, and loadings.

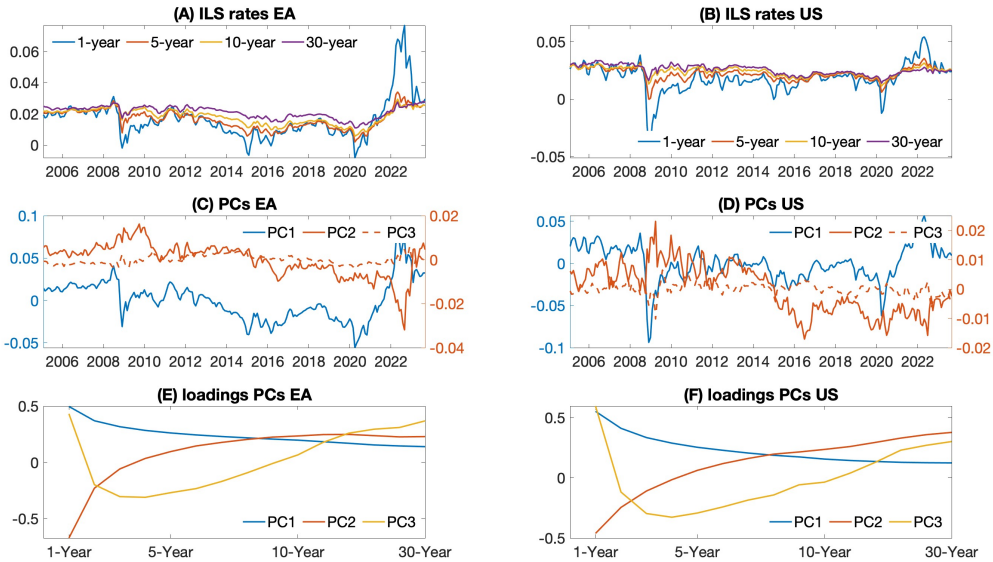

Notes: Panel A (B) plots the EA (US) ILS rates with maturities of 1, 5, 10, and 30 years. Panel C (D) depicts the first three principal components of all the EA (US) ILS rates, while Panel E (F) reports their respective loadings.

For both ILS term structures, the loadings of the first factor are the (exponentially decaying) weighted averages of all ILS rates, while the second factors load negatively on short-term maturities and positively on long-term ones, giving them the interpretation

of level and slope factors. The third factor is the difference between (i) the average of long- and short-term ILS rates and (ii) medium-term ones, i.e., the common shape of yield curve curvature factors. By summing up the weights for each factor/country, i.e., w_l, w_s, and w_c, the resulting entries for the cointegration matrices $\mathbf{\Gamma^p}$s of equation (13b) are:

$$\mathbf{\Gamma}^{\mathbf{p},EA} = \begin{bmatrix} 3.8 & 0 \\ 0.8 & 0 \\ 0.3 & 0 \end{bmatrix}, \quad \mathbf{\Gamma}^{\mathbf{p},US} = \begin{bmatrix} 3.5 & 0 \\ 1.6 & 0 \\ -0.1 & 0 \end{bmatrix}.$$

3.1.2 Macroeconomic and survey data

Macroeconomic data.
Macroeconomic variables are divided into international and country-specific factors. The international factors are (i) the Kilian (2009) index of global real economic activity (percent deviation from trend) and (ii) the monthly log of real oil price (spot), i.e., the West Texas Intermediate (WTI), for the US, and Bloomberg European Dated Brent Forties Oseberg Ekofisk (BFOE) Crude Oil Spot Price the Crude Oil Prices: Brent - Europe, for the EA, both deflated by the respective local consumer price indexes.[7]

Country-specific factors are obtained from the Federal Reserve Economic Data (FRED) database maintained by the Federal Reserve Bank of St. Louis for the US and from the ECB Data Portal for the EA.[8] We proxy the inflation factor via the month-on-month growth rate of the inflation index underlying the ILS contracts, i.e., the seasonally-adjusted Harmonised Index of Consumer Prices (HICP) excluding tobacco for the EA and the Consumer Price Index (CPI) for the US, while the month-on-month growth rate of the Industrial Production Index gives the real activity measure.[9] As risk-free rates, we use the one-year T-bill rate for the US and the one-year OIS rate for the EA.

[7] The results are equivalent when using nominal oil prices instead.

[8] The data codes are listed in Section A.1.

[9] We find similar results with the following local EA inflation measures: (i) the HICP excluding energy and food (ICP.M.U2.Y.XEF000.3.INX) and (ii) the HICP - All-items.

Figure 2: Observable variables

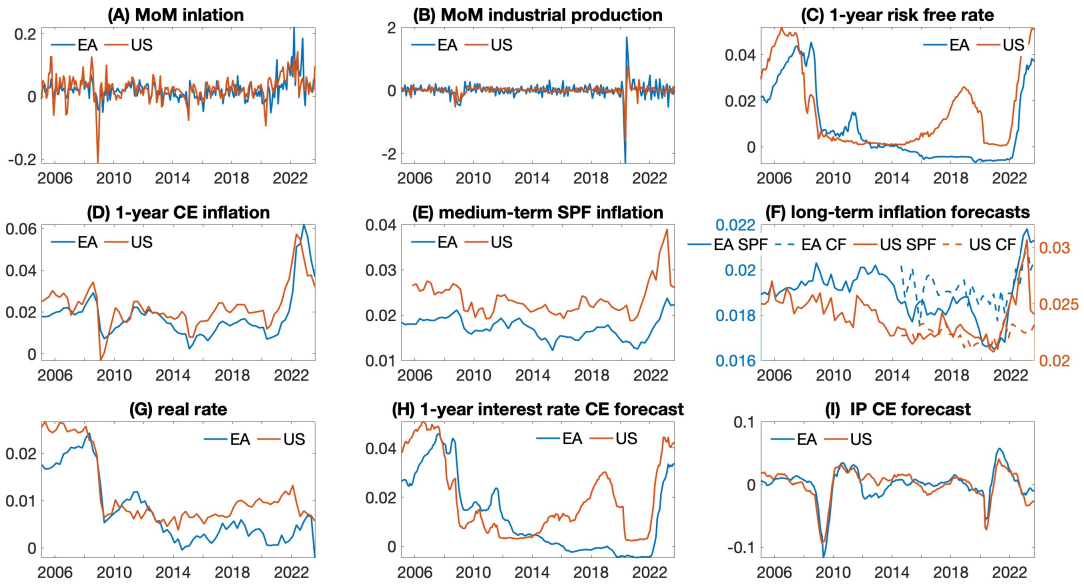

Notes: The top panels report the observed series of month-on-month inflation, industrial production growth (panels A and B, respectively), and the one-year risk-free rate (panel C). The middle panels depict the inflation surveys. Panel D plots the monthly Consensus Economics (CE) one-year-ahead inflation forecast, panel E reports the two (five) year inflation Survey of Professional Forecast (SPF) for the EA (US), and panel F depicts (i) the five (ten) year inflation forecast from the SPF for the EA (US), and (ii) the long-term (above five years) CE inflation forecasts. Finally, the bottom panels show the quarterly Holston et al. (2017) natural rate of interest (panel G), and the monthly CE one-year risk-free rate (panel H) and industrial production (panel I) forecast. In each panel, blue lines refer to EA data, while red lines are for US data.

Surveys and model-based series.
Finally, we exploit the information contained in surveys, and we employ the quarterly natural interest rate constructed by Holston et al. (2017) to (i) identify the two stochastic trends and (ii) identify the value of real activity at the beginning of the COVID-19 period.

To fix notations, the surveys forecasts for a variable x are labelled as $\mathbb{E}_t^{\mathcal{S}} x_{t+t_1 \to t+t_2}$, where (i) $\mathcal{S}$ indicates the source from where the subjective forecasts are obtained, and (ii) $t+t_1$ and $t+t_2$ are the beginning and the end of the forecasting period, respectively, expressed in months. For each country, we use two survey providers: the Survey of Professional Forecasters (SPF) and the Consensus Economics (CE) forecasts, i.e., $\mathcal{S} = \{SPF, CE\}$. The European Central Bank (ECB) provides the EA SPF, while the Philadelphia Federal Reserve provides the US SPF. From the ECB (Philadelphia FED) SPFs, we select the year-on-year inflation forecast in two and five years (average inflation over the next five and ten years), which we label $\mathbb{E}_t^{\text{SPF}} \pi_{t+t_1 \to t+t_2}$, with $t_1 = \{12, 48\}$ and $t_2 = \{24, 60\}$ ($t_1 = \{1, 1\}$ and $t_2 = \{60, 120\}$) months.We use two sets of CE surveys, the short-term and long-term forecasts. Short-term CE forecasts for the next-year inflation rate, $\mathbb{E}_t^{\text{CE}} \pi_{t+1 \to t+12}$, industrial production, $\mathbb{E}_t^{\text{CE}} g_{t+1 \to t+12}$, and one-year interest rates, $\mathbb{E}_t^{\text{CE}} i_{t+1 \to t+12}$, are proxied by an extrapolation from (i) the current and next calendar year forecasts and (ii) from the next-year forecast for the 3-month and 10-year interest rates,

respectively:

$$\mathbb{E}_t^{\text{CE}}\pi_{t+1\to t+12} = \frac{(13-\mathsf{m}(t))-1}{12}\mathbb{E}_t^{\text{CE}}\pi_{\mathsf{y}(t)} + \frac{(\mathsf{m}(t)-1)}{12}\mathbb{E}_t^{\text{CE}}\pi_{\mathsf{y}(t)+1} \tag{25a}$$

$$\mathbb{E}_t^{\text{CE}}g_{t+1\to t+12} = \frac{(13-\mathsf{m}(t)-1)}{12}\mathbb{E}_t^{\text{CE}}g_{\mathsf{y}(t)} + \frac{(\mathsf{m}(t)-1)}{12}\mathbb{E}_t^{\text{CE}}g_{\mathsf{y}(t)+1} \tag{25b}$$

$$\mathbb{E}_t^{\text{CE}}i_{t+12} = \mathbb{E}^{\text{CE}}i^{3}_{t+12} + \frac{\mathbb{E}_t^{\text{CE}}i^{120}_{t+12} - \mathbb{E}_t^{\text{CE}}i^{3}_{t+12}}{120-3}(12-3). \tag{25c}$$

In equations (25a) and (25b), $\mathsf{y}(t)$ and $\mathsf{m}(t)$ are the calendar years and months related to time t, respectively. The expression approximates fixed-horizon forecasts as a weighted average of fixed-event forecasts (see Dovern et al., 2012). Equation (25c) approximates the forecast of the 1-year interest rate, $\mathbb{E}_t^{\text{CE}}i_{t+12}$, as the weighted average of the forecast of the 3-month and 10-year interest rates in one year, $\mathbb{E}_t^{\text{CE}}i^{3}_{t+12}$ and $\mathbb{E}_t^{\text{CE}}i^{120}_{t+12}$, respectively. The implicit assumption is that the forecasters-implied yield curve has the same slope for all maturities. Long-term CE forecasts are short-term interest rates and inflation expectations in five to ten years, $\mathbb{E}_t^{\text{CE}}i^{3}_{t+60\to t+120}$ and $\mathbb{E}_t^{\text{CE}}\pi_{t+60\to t+120}$. Finally, our last observed variable is the quarterly natural interest rate constructed by Holston et al. (2017), $\tilde{r}^*_t$, which helps identify the stochastic trend for the interest rate.

3.2 Estimation strategy

The estimation of our term structure model involves two steps: (i) the identification of the stochastic trends and the fitting of risk factors' dynamic system (17) and (ii) the pricing of the ILS contracts via the multivariate version of equation (20). The first step is performed in a state-space setting, while the second maximizes the fit of ILS rates via (a constrained) linear system. We estimate the system outlined in Section 2.2 via a state-space setting, whereby the state variables, $\mathcal{Z}_t$, see (17), are linearly related to a set of observable variables, $\mathcal{Y}_t$:

$$\mathcal{Y}_t = \mathbf{a} + \mathbf{B}\mathcal{Z}_t + \mathbf{\Sigma}^{\mathcal{Y}}\boldsymbol{\epsilon}^{\mathcal{Y}}_t, \quad \boldsymbol{\epsilon}^{\mathcal{Y}}_t \sim \mathcal{N}(\mathbf{0}, \boldsymbol{I}), \tag{26}$$

where $\mathbf{\Sigma}^{\mathcal{Y}}$ is a diagonal matrix of standard deviations. The observed series and their corresponding loadings, $\mathbf{a}$ and $\mathbf{B}$, are divided in four blocks:

$$\mathcal{Y}'_t = \begin{bmatrix}\mathcal{Y}^{\mathcal{O}'}_t & \mathcal{Y}^{\pi'}_t & \mathcal{Y}^{g'}_t & \mathcal{Y}^{i'}_t\end{bmatrix} \tag{27a}$$

$$\mathbf{a}' = \begin{bmatrix}\mathbf{a}^{\mathcal{O}'} & \mathbf{a}^{\pi'} & \mathbf{a}^{g'} & \mathbf{a}^{i'}\end{bmatrix} \tag{27b}$$

$$\mathbf{B}' = \begin{bmatrix}\mathbf{B}^{\mathcal{O}'} & \mathbf{B}^{\pi'} & \mathbf{B}^{g'} & \mathbf{B}^{i'}\end{bmatrix}. \tag{27c}$$

The first block, $\mathcal{Y}^{\mathcal{O}}_t$, includes the observed data, i.e. $\mathbf{w}_t$, $\mathbf{m}_t$, and $\mathbf{p}_t$:

$$\mathcal{Y}^{\mathcal{O}}_t = \begin{bmatrix}p^{o}_t & g^{w}_t & \pi_t & g_t & i_t & l_t & s_t & c_t\end{bmatrix}' \tag{28a}$$

$$\mathbf{a}^{\mathcal{O}} = \begin{bmatrix}0 & 0 & 0 & 0 & 0 & 0 & 0 & 0\end{bmatrix}' \tag{28b}$$

$$\mathbf{B}^{\mathcal{O}} = \begin{bmatrix}\iota^{\Delta p^{o\prime}} & \iota^{g^{w\prime}} & \iota^{\pi'} & \iota^{g'} & \iota^{i'} & \iota^{l'} & \iota^{s'} & \iota^{s'}\end{bmatrix}'. \tag{28c}$$

Since the stationary state variables are observed without error, the elements of $\mathbf{a}^{\mathcal{O}}$ are set to zero while $\mathbf{B}^{\mathcal{O}}$ is made of row vectors selecting the respective observed variables from the state vector, $\mathcal{Z}_t$. For example, for the macro series, these restrictions correspond to:

$$\iota^{\pi} = \begin{bmatrix} 0 & 0 & 1 & 0 & 0 & 0 & ... & 0 \end{bmatrix} \tag{29a}$$

$$\iota^{g} = \begin{bmatrix} 0 & 0 & 0 & 1 & 0 & 0 & ... & 0 \end{bmatrix} \tag{29b}$$

$$\iota^{i} = \begin{bmatrix} 0 & 0 & 0 & 0 & 1 & 0 & ... & 0 \end{bmatrix}. \tag{29c}$$

To account for the large deviation of the industrial production series at the beginning of the COVID-19 period, we impose that g_t is not observed from March 2020 to August 2020. The third block, see infra, identifies g_t over that period. The second block includes the four inflation survey data from the SPF and from the CF:

$$\mathcal{Y}_t^{\pi} = \begin{bmatrix} \mathbb{E}_t^{\text{SPF}} \pi_{t+t_1 \to t+t_2} & \mathbb{E}_t^{\text{SPF}} \pi_{t+t_3 \to t+t_4} & \mathbb{E}_t^{\text{CE}} \pi_{t+1 \to t+12} & \mathbb{E}_t^{\text{CE}} \pi_{t+61 \to t+120} \end{bmatrix}' \tag{30a}$$

$$\mathbf{a}^{\pi} = \begin{bmatrix} \iota^{\pi} \bar{\mathbf{a}}_{t_1 \to t_2} & \iota^{\pi} \bar{\mathbf{a}}_{t_3 \to t_4} & \iota^{\pi} \bar{\mathbf{a}}_{1 \to 12} & \iota^{\pi} \bar{\mathbf{a}}_{61 \to 120} \end{bmatrix}' \tag{30b}$$

$$\mathbf{B}^{\pi} = \begin{bmatrix} \iota^{\pi} \bar{\mathbf{B}}'_{t_1 \to t_2} & \iota^{\pi} \bar{\mathbf{B}}'_{t_3 \to t_4} & \iota^{\pi} \bar{\mathbf{B}}'_{1 \to 12} & \iota^{\pi} \bar{\mathbf{B}}'_{61 \to 120} \end{bmatrix}', \tag{30c}$$

where (i) for the EA (US) t_1, t_2, t_3, and t_4 are equal to 12, 24, 48, and 60 months (1, 60, 1, and 120 months), respectively, and ι^{π}, defined in (29a) selects the inflation components of $\bar{\mathbf{a}}'_{\tau_1 \to \tau_2}$ and $\bar{\mathbf{B}}'_{\tau_1 \to \tau_2}$. For a generic forecasting horizon ranging from τ_1 to τ_2, the loadings $\bar{\mathbf{a}}'_{\tau_1 \to \tau_2}$ and $\bar{\mathbf{B}}'_{\tau_1 \to \tau_2}$ are the model-implied average forecasts of the state variables over the period $[\tau_1, \tau_2]$:

$$\bar{\mathbf{a}}_{\tau_1 \to \tau_2} = \frac{1}{\tau_2 - \tau_1 + 1} \sum_{H=\tau_1}^{\tau_2} \left[\sum_{h=1}^{H} \mathbf{\Phi}^{h-1} \right] \boldsymbol{\mu} \tag{31a}$$

$$\bar{\mathbf{B}}_{\tau_1 \to \tau_2} = \frac{1}{\tau_2 - \tau_1 + 1} \sum_{H=\tau_1}^{\tau_2} \mathbf{\Phi}^{H}. \tag{31b}$$

As we observed that the 12-month CE forecasts were substantially more volatile than the SPF's, we (i) scale its model-implied counterpart by a factor β^{CE} and (ii) we add to it a level factor, α^{CE}, to account for shifts in the level of the model-implied forecast brought about by the scaling factor β^{CE}.

The third block includes information related to industrial production around the first period of the COVID-19 crisis, from March 2020 to August 2020. During this period, we treat the series of Industrial Production Indexes as a latent factor which is noisily observed via (i) the realized month-on-month growth rate of the Industrial Production Index from March 2020 to August 2021 and (ii) its year-on-year CE forecast, $\mathbb{E}_t^{\text{CE}} g_{t+12}$. The resulting measured variables and loadings are:

$$\mathcal{Y}_t^{g} = \begin{bmatrix} \tilde{g}_t & \mathbb{E}_t^{\text{CE}} \tilde{g}_{t+1 \to t+12} \end{bmatrix}' \tag{32a}$$

$$\mathbf{a}^{g} = \begin{bmatrix} \alpha^{\tilde{g}} & \iota^{g} \bar{\mathbf{a}}_{1 \to 12} \end{bmatrix}' \tag{32b}$$

$$\mathbf{B}^{g} = \begin{bmatrix} \beta^{\tilde{g}} \iota^{g} & \iota^{g} \bar{\mathbf{B}}'_{1 \to 12} \end{bmatrix}', \tag{32c}$$

where the parameters $\alpha^{\tilde{g}}$ and $\beta^{\tilde{g}}$ allow the observed industrial production growth to differ from the latent one, the loadings $\bar{\mathbf{a}}_{1\to12}$ and $\bar{\mathbf{B}}_{1\to12}$ are from equations (31a) and (31b), and ι^{g} is defined in equation (29b).

The last block, $\mathcal{Y}_t^i$, includes three types of information, coming from two sources: (i) the short- and long-term CE interest rates forecasts, and (ii) the Holston et al. (2017) measure of the equilibrium real rate. The resulting block of the measurement equations includes:

$$\mathcal{Y}_t^i = \begin{bmatrix} \mathbb{E}_t^{\text{CE}} i_{t+12}^{12} & \mathbb{E}_t^{\text{CE}} i_{t+61\to t+120}^{12} & \tilde{r}_t^* \end{bmatrix}' \tag{33a}$$

$$\mathbf{a}^i = \begin{bmatrix} \iota^i \bar{\mathbf{a}}_{12} & \iota^i \bar{\mathbf{a}}_{61\to120} & \alpha^{\tilde{r}} \end{bmatrix}' \tag{33b}$$

$$\mathbf{B}^i = \begin{bmatrix} \iota^i \bar{\mathbf{B}}'_{12} & \iota^i \bar{\mathbf{B}}'_{61\to120} & \beta^{\tilde{r}} \end{bmatrix}', \tag{33c}$$

where the loading of the interest forecasts are obtained via the equations (31a) and (31b), while $\alpha^{\tilde{r}}$ and $\beta^{\tilde{r}}$ account for potential differences in mean and volatility between our model-implied stochastic trend for the real rate and the Holston et al. (2017)'s measure. Finally, given the identifying assumption related to the measurement equation, the matrix with the standard deviations of its errors is defined as:

$$\mathbf{\Sigma}^{\mathcal{Y}} = \text{diag}\begin{bmatrix} 0 & \sigma^{g} & \sigma^{\text{SPF}_1^{\pi}} & \dots & \sigma^{\tilde{r}} \end{bmatrix},$$

with all non-zero elements except for the observed inflation and short-term interest rate equations.

Likelihood function.

We estimate the model composed by equations (26) and (17) using a penalized likelihood approach, a method that is widely used in high-dimensional statistical modeling (see Tibshirani, 1996; Fan and Li, 2001, among others). The penalized log-likelihood is composed of two parts:

$$l \propto \underbrace{-\frac{1}{2}\sum_{t=\Upsilon}^{T}(\ln|\boldsymbol{F}_t| + \boldsymbol{v}_t'\boldsymbol{F}_t^{-1}\boldsymbol{v}_t)}_{\text{KF-EPD}} + \underbrace{p(\mathbf{\Phi}) + p(\mathbf{\Sigma}^{\xi}) + p(\mathbf{\Sigma}^{\mathcal{Y}}) + p(\alpha) + p(\beta)}_{\text{Penalty}}. \tag{34}$$

The component labeled KF-EPD is obtained by exploiting the Gaussian nature of the linear state-space model. It represents the sum of the likelihood of the Kalman Filter's prediction errors, $\boldsymbol{v}_t$, whose variance is given by $\boldsymbol{F}_t$. The functional forms of $\boldsymbol{v}_t$ and $\boldsymbol{F}_t$ derive from the Kalman Filter's recursions (Harvey, 1990, page 125).

The second part of the log-likelihood includes the penalties for the system's (block of) parameters. The first set of penalties relates to the elements of $\mathbf{\Phi}$. For these parameters, we adopt a $\|\text{L}\|^2$ regularization, whereby the (scaled) elements of $\mathbf{\Phi}$ are shrunk to zero via the following quadratic penalty function:

$$p(\mathbf{\Phi}) = \sum_{\upsilon=1}^{\Upsilon}\sum_{j=1}^{3}\sum_{i=1}^{3}\lambda_{\upsilon}(i,j)\left[\upsilon\frac{\tilde{\phi}_{\upsilon}(i,j)}{\varphi_{i,j}}\right]^2, \quad \lambda_{\upsilon}(i,j) = \begin{cases} \zeta_1^2 & \forall i = j \\ \zeta_1^2\zeta_2^2 & \text{otherwise.} \end{cases} \tag{35}$$

In equation (35), the interpretation and values of the scaling coefficients $\varphi_{i,j}$, ζ_1, and ζ_2 are as follows. The coefficients $\varphi_{i,j}$ account for the fact that the macro series are not

standardized and might thus have different sample variances. We set their values to the outer product of the standard deviations of $\hat{\mathbf{m}}_t$, the deviation of the macro variables from the stochastic trends extrapolated from the surveys series. To penalize model complexity, we divided $\varphi_{i,j}$ by the lag of the coefficients it refers to, implying stronger regularization for additional lags added to the model. The coefficients ζ_1 and ζ_2 control the overall shrinkage and the penalization for the interaction coefficients, respectively. Following the Bayesian literature, we set their values to $\zeta_1 = \zeta_2 = \sqrt{2}$.

The additional penalties relate to the identification of the stochastic trends. They are linked to (i) the standard deviations of the stochastic trends, $\boldsymbol{\Sigma}^{\xi}$, and of the measurement equation (26), $\boldsymbol{\Sigma}^{y}$, and (ii) to the additional coefficients of the measurement equations, namely α^{CE}, β^{CE}, $\alpha^{\tilde{g}}$, $\beta^{\tilde{g}}$, $\alpha^{\tilde{g}}$, $\beta^{\tilde{g}}$, $\alpha^{\tilde{r}}$, and $\beta^{\tilde{r}}$. For the standard deviations, we use the following penalty function:

$$p(\boldsymbol{\sigma}^k) = \lambda^k \left[\ln \boldsymbol{\sigma}^k - \ln \bar{\boldsymbol{\sigma}}^k\right]^2, \quad \{\lambda^k, \ln \bar{\boldsymbol{\sigma}}^k\} = \begin{cases} \{100, \ln \hat{\boldsymbol{\sigma}}^k\} & \forall k = \pi^*, r^* \\ \{1, -5\} & \text{otherwise,} \end{cases} \tag{36}$$

where $\bar{\boldsymbol{\sigma}}^{\pi^*}$ and $\bar{\boldsymbol{\sigma}}^{r^*}$ are extrapolated from the 2-year SPF and Holston et al. (2017)'s measure, respectively. Intuitively, the penalties on equation (36) shrink the estimated parameters toward $\ln \hat{\boldsymbol{\sigma}}^k$, whereby a deviation from these centered values are penalized by a factor λ^k. Our penalty functions assign a great deal of importance to the survey information to the Holston et al. (2017)'s measure of the real rate, as it is highlighted by the values of $\ln \hat{\boldsymbol{\sigma}}^k$, which are relatively small or equal to their extrapolated values, and by the high values assigned to λ^k. For the additional coefficients of the measurement equations, we adopt the following penalty:

$$p(\boldsymbol{\theta}^k) = \lambda^k \left[\boldsymbol{\theta}^k - \bar{\boldsymbol{\theta}}^k\right]^2, \quad \{\lambda^k, \bar{\boldsymbol{\theta}}^k\} = \begin{cases} \{1, 0\} & \forall \theta = \alpha \\ \{\frac{1}{\sqrt{.5}}, 3\} & \theta = \beta \wedge k = \tilde{g} \\ \{\frac{1}{\sqrt{.1}}, 3\} & \theta = \beta \wedge k = r^* \\ \{1, 1\} & \text{otherwise} \end{cases}. \tag{37}$$

Equation (37) centers the parameters α and β around zero and one, implying that we start from the assumption that the information provided by the observed series is unbiased. The only exception is the coefficient $\beta^{\tilde{g}}$, which we center around 3 to acknowledge that the observed value of industrial production might be more volatile than our latent series.

3.2.1 Term structure model

We estimate the parameters of equation (20) using a quasi-maximum likelihood procedure. Specifically, we fix the parameters $\boldsymbol{\mu}^{\mathbb{P}}$ and $\boldsymbol{\Phi}^{\mathbb{P}}$ of (17) and we estimate the parameters $\boldsymbol{\mu}^{\mathcal{X}}$, $\boldsymbol{\Phi}^{\mathcal{X}}$ and $\boldsymbol{\Sigma}^{\boldsymbol{p}}$ by fitting the term structure of the ILS rates. As in Joslin et al. (2011), the starting point for the estimation of $\boldsymbol{\Sigma}^{\boldsymbol{p}}$ are the state-space estimates. We maximize the likelihood function by combining simulated annealing and a simplex procedure.

4 Empirical Results

In what follows, we focus on decomposing ILS rates in expected and inflation risk premium components. We present the results for a model with three lags. Appendix A.3 reports

the parameters estimates, the plot of the stochastic trends, and the fit of the measurement equation. The t-statistics and confidence intervals are based on 500 bootstrapped samples obtained as in Stoffer and Wall (1991). We focus our analysis on the 2-year (short-term) and 10-year (long-term) contracts, which are maturities also analyzed by studies employing ILS data (Haubrich et al., 2012; Berardi and Plazzi, 2018) and TIPS data (Breach et al., 2020).

4.1 Expected components and inflation risk premia

This section analyzes the decomposition of the two- and ten-year ILS rates in EC and IRP. Panel a (b) of Figure 3 reports the evolution of the 2-year (10-year) ILS rates and its EC and ILS decompositions for the US (sub panel A) and the EA (sub panel B). Table A6 in the appendix reports the summary statistics of the EC and TP components for the full sample and the pre-January 2022 sample.

Expected component (EC).
As in Berardi and Plazzi (2018), we find that US short-term expectations – proxied by the EC of the ILS rates – are relatively volatile, fluctuating between -32 and 311 bps. Furthermore, on average, they are comparable to other EC measures extracted from the ILS contract. For example, over the period 2009-2015, our average two-year expected inflation is comparable to the estimates of Fleckenstein et al. (2017) (only 10 bps smaller), albeit it is roughly twice more volatile with a standard deviation of 22 bps against 41 bps. The most volatile periods relate to the Great Financial Crisis (GFC), the COVID-19 period, and the Ukraine war, reflecting the market's fear of the possibility of a prolonged recession (GFC and early stage of COVID-19) and the fear of high inflation brought about by supply chain bottlenecks, geopolitical tensions, and large fiscal stimulus packages (last part of COVID-19 crisis and Ukraine war). The EC of the short-term ILS rates for the EA are considerably more volatile than their US counterparts, with a 30% higher standard deviation. The 2-year EA EC fluctuates between 58 and 455 bps, and a significant portion of this variation can be attributed to the recent Ukraine war, which has caused the short-term EC in the EA to nearly double in terms of volatility, rising from 37 to 65 bps.

Turning to longer-term EC, two observations stand out. First, they are substantially less volatile than their short-term counterparts. For example, in the EA (US), the standard deviation of the 10-year EC is roughly one-quarter (one-third) of the 2-year analog. This finding is also documented in the literature. For example, Fleckenstein et al. (2017) find that in the US, the standard deviation of the 10-year EC of ILS is a fraction (one-third) of the 2-year counterpart while Berardi and Plazzi (2018) document that long-term expectations are quite stable and fluctuate within the range 115-215 bps, which is slightly lower than our 157-261 bps estimates (which include the recent period of high inflation). Second, despite a more volatile EC in the short end, the long-term EA EC is less volatile than its US counterpart. Potentially, the latter observation might reflect that, in contrast to the dual mandate of the FED, the ECB's mandate focuses primarily on inflation stabilization. However, as risk premia have been persistently negative between 2013 and 2021 for some segments of the ILS markets, a careful reading of inflation swaps is needed to draw firm conclusions regarding the anchoring of inflation expectations in the EA during that period.

Figure 3: 2-year and 10-year rates, expected and inflation risk premia components

(a) 2 years ILS contract

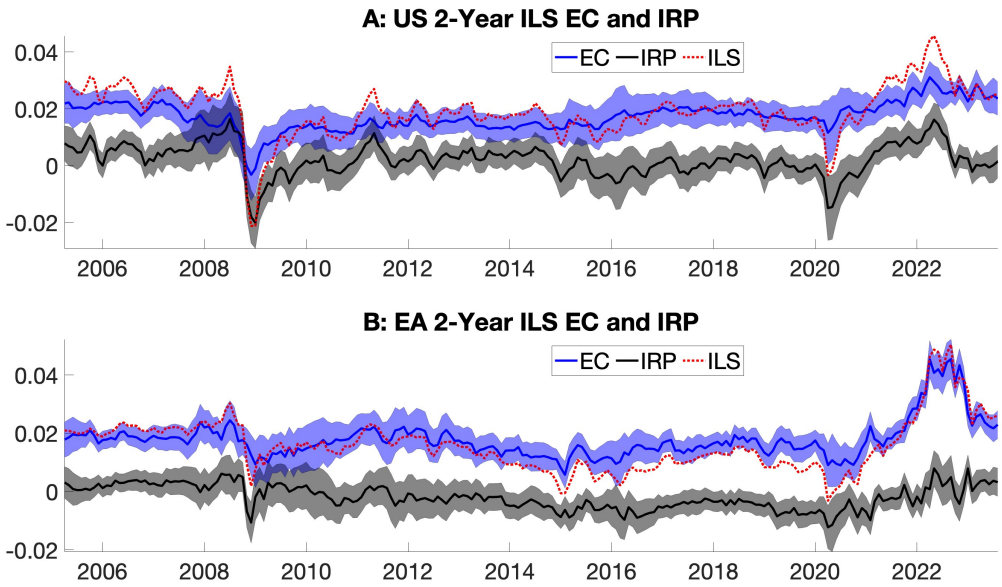

(b) 10 years ILS contract

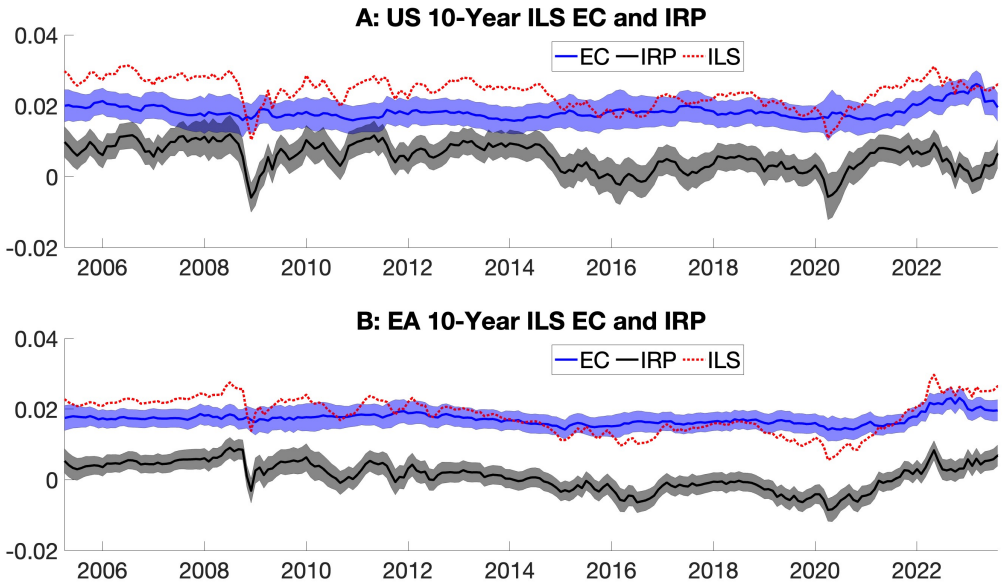

Notes: *Panel (a)*: for the 2-year ILS rates, the (sub) panel A (B) of this figure reports the US (EA) ILS rates, and their decompositions in EC (blue) and IRP (grey). *Panel (b)*: this panel reproduces similar plots to panel (a) but for a 10-year ILS rate. Shaded areas indicate the 95% confidence intervals.

Inflation risk premium (IRP).
The short-term US inflation risk premium fluctuates between -202 and 164 bps, with the most abrupt changes happening around Lehman's default when it dropped by roughly 320 bps over four months. It matches Fleckenstein et al. (2017) averages – and references therein – but is five times more volatile. It was positive before the GFC, a period characterized by relatively stable inflation and growth perspectives; see Figure 2. The

deterioration in (expected) economic conditions, associated with the low inflation outlook, contributed to the flip in the sign of the inflation risk premium at the end of 2008. Similarly to Haubrich et al. (2012), the risk premia fluctuated in negative territory until the end of 2010. However, in the latter part of the period, negative premia might have been brought about by the post-crisis recovery of the US economy and the return of inflation to its pre-crisis levels. In the succeeding period, the US inflation risk premia turned negative around the 2010s oil price glut, which was combined with the mini-recession of 2015, and from mid-2019 until the end of 2020, a period characterized first by less-than-expected economic growth, and then by the COVID-19 crisis. Our results corroborate the findings of Fleckenstein et al. (2017), Haubrich et al. (2012), and Camba-Mendez and Werner (2017), who suggest that (i) around the GFC and the oil price glut, the probability of deflation might be as high as 30% for a 2-year horizon (contract), that (ii) the two-year IRP was substantially negative during the GFC, and that (iii) short-term US IRP can be negative for a prolonged period.

The short-term EA inflation risk premium varies between -122 and 80 bps and is, on average, negative. It was positive prior to the GFC but turned negative after its inception. In contrast to the US case, EA risk premia did not fall as much and quickly reverted to positive values. Berardi and Plazzi (2018) show that volatility and IRP are negatively related in periods of crisis or market-wide distress. Hence, the quick flip in the sign of EA risk premia is potentially due to the region's lower volatility of inflation (and its projections). From the beginning of 2013, risk premia started to decline and turned negative for a prolonged period until the 2022 Russian invasion of Ukraine. This period coincides with the so-called EA lowflation, during which a benign economic recovery coincided with inflation remaining persistently weak and below the ECB's then-prevailing inflation aim of below, but close to, 2% in the medium term (Stevens and Wauters, 2021). The decline in risk premia intensified around the oil price glut and, after a partial recovery in 2018, reached their lowest levels when the COVID-19 crisis erupted.

In both areas, the 10-year maturity IRP is, on average, positive and more volatile than the EC. This result is standard for the US and is found elsewhere in the literature; see, for example, Fleckenstein et al. (2017) and Haubrich et al. (2012) for studies using alternative approaches with a comparable dataset. Our IRP is 30% more volatile than the estimates of Fleckenstein et al. (2017), and its mean lies between their 22 bps estimates and the 67 bps and 115 bps averages of Chernov and Mueller (2012) and Campbell and Viceira (2001), respectively. The longer-term IRP is negative only in three episodes – the GFC, the oil glut, and the COVID-19 crisis (in the EA, the IRP was also negative before that period) – and for only a short period. For the EA, over the period January 2012 - July 2018, Böninghausen et al. (2018) find a similar pattern for the market-based long-term IRP, attributing most of the fall in (5-year) ILS rates (in 5 years) over the period from 2014 to 2016 to deflation risk. The higher volatility implies that most of the variation in longer-term ILS rates, see Table 1, comes from IRP's movements.[10] From the COVID-19 crisis onward, we observe an increase in the long-term EA IRP. This finding relates to Mouabbi et al. (2023), who document a rising contribution of adverse supply shocks to inflation and a significant decrease in the correlation between inflation and economic activity. Applying the terminology of Cieslak and Pflueger (2023), this could be considered as the beginning of a period of "bad inflation," wherein supply-driven inflation dynamics result in positive long-term (bond) risk premiums.

[10]Decomposing the ILS volatility into the EC, IRP, and correlation component highlight that for the EA (US) 72% (90%) of 10-year ILS volatility is due to the IRP component.

Figure A3 in the appendix reports the deterministic components for the US (EA) 2-year and 10-year ILS rates and their decomposition in EC and IRP parts, respectively, based on our model specification (top panels) and a "latent" model with only the three principal components as risk factors (bottom panels). Giannone et al. (2019) point out that it is important to discipline the long-run behavior of vector autoregression models. Otherwise, the deterministic components might, implausibly, capture a large share of the variation in the observed time series. Our model can produce deterministic components of the ILS rates that are not influenced by its low-frequency movements. This contrasts with the results obtained from a three-factor latent model, whereby for the EA, the deterministic components of the ILS rates display oscillating behavior, especially for the 2-year ILS rates, to explain a share of the low-frequency variability observed in the data. The problem is pronounced for models estimated before the Ukraine crisis (dotted lines).

4.2 Variance decomposition.

We report the variance decomposition of the 2-year and 10-year US (EA) ILS rates, its expected and IRP components, in panels A to C (D to F) of Table 2, respectively. We aggregate the shocks in four groups: (i) Σ_{PCs}, which refers to the *principal components* of the yield curve and is the sum of level, slope, and curvature innovations; (ii) Σ_{Gl}, namely the sum of oil and *global* real activity innovations; (iii) Σ_{Loc} representing the sum of the *local* macro variable innovations (month-on-month inflation, month-on-month industrial production growth, and the one-year risk-free rate); and (iv) the sum of *long-run* innovations (inflation and real rate trends), labeled Σ_{LR}.

The stochastic variation in ILS rates in both regions is influenced by short-term and long-term economic innovations, with varying contributions depending on the contract's maturity and the frequency of the movements being analyzed. We first focus on the short-term ILS contracts. Our model reveals that transitory economic developments drive high-frequency movements (12-month horizon) in the 2-year ILS rates. However, the extent to which local and international factors contribute to these movements differs between regions. In the US, international innovations account for most stochastic variation (35% in total, compared to 27% for local economic factors). In contrast, in the EA, local economic innovations contribute to approximately half of the total movements.

When analyzing low-frequency movements of ILS rates (10-year horizon), a more fragmented picture emerges across the two regions. In the US, short-term rates are less influenced by transitory economic innovations, which explain only about one-third of the total variation, while long-term innovations play a crucial role, accounting for half of the total ILS low-frequency variation. Conversely, in the EA, transitory economic innovations account for 67%, while long-term factors contribute only 10% of the total variation.

A closer examination of the decomposition of ILS rates reveals three key patterns. First, in the US, international factors primarily impact ILS rates through the IRP channel, while in the EA, local factors are the most important economic drivers of both the IRP and the EC. In the US, two-thirds of IRP variation can be attributed to international innovations, while for the EA, local factors account for around one-third (half) of the IRP (EC) fluctuations.

Second, long-term economic trends significantly impact the low-frequency movement of the EC, particularly in the US, where stochastic trend innovations explain three-quarters of the total variation, compared to one-quarter in the EA. Finally, local economic innovations are mainly associated with variation in the EC of short-term ILS rates, es-

pecially in the EA, where they account for at least 60% of total variation. The variance decomposition of the 10-year maturity indicates that, for both areas, long-run innovations play a larger role in explaining the movements of longer-term ILS rates compared to short-term contracts. This result is particularly pronounced for low-frequency movements, whereby innovations in stochastic trends account for more than 80% and 20% of the variation in US and EA rates, respectively. The EC is the channel mostly linked to long-term innovations, with more than 95% (85%) of the US (EA) variation attributed to long-run innovations. Next, we quantify how innovations in short and long-term variables influence ILS rates throughout recent episodes of interest.

Table 2: Error variance decomposition

US

		A: ILS level				B: Expected component				C: Inflation risk premia			
Maturity	Horizon	Σ_{PCs}	Σ_{Gl}	Σ_{Loc}	Σ_{LR}	Σ_{PCs}	Σ_{Gl}	Σ_{Loc}	Σ_{LR}	Σ_{PCs}	Σ_{Gl}	Σ_{Loc}	Σ_{LR}
2-year	12M	0.33	0.35	0.27	0.05	0.20	0.12	0.40	0.28	0.19	0.65	0.13	0.03
2-year	120M	0.15	0.19	0.14	0.52	0.04	0.12	0.10	0.74	0.18	0.66	0.13	0.03
10-year	12M	0.30	0.32	0.13	0.25	0.02	0.05	0.06	0.87	0.28	0.55	0.06	0.12
10-year	120M	0.06	0.07	0.03	0.84	0.00	0.02	0.01	0.97	0.21	0.62	0.06	0.11

EA

		D: ILS level				E: Expected component				F: Inflation risk premia			
Maturity	Horizon	Σ_{PCs}	Σ_{Gl}	Σ_{Loc}	Σ_{LR}	Σ_{PCs}	Σ_{Gl}	Σ_{Loc}	Σ_{LR}	Σ_{PCs}	Σ_{Gl}	Σ_{Loc}	Σ_{LR}
2-year	12M	0.26	0.22	0.52	0.00	0.12	0.20	0.64	0.04	0.47	0.15	0.33	0.04
2-year	120M	0.23	0.23	0.44	0.10	0.09	0.16	0.49	0.27	0.45	0.21	0.27	0.07
10-year	12M	0.49	0.19	0.31	0.01	0.07	0.10	0.35	0.48	0.59	0.16	0.21	0.05
10-year	120M	0.38	0.18	0.22	0.22	0.02	0.02	0.07	0.89	0.55	0.19	0.19	0.07

Notes: For a 2-year and 10-year US (EA) ILS contract panels A to C (D to F) report the error variance decomposition of the ILS rate level, the EC, and inflation risk premia, respectively. Innovations are grouped as: (i) Σ_{PCs}, which is the sum of level, slope, and curvature innovations; (ii) Σ_{Gl}, namely the sum of oil and global real activity innovations; (iii) Σ_{Loc} representing the sum of the local macro variable innovations (month-on-month inflation, month-on-month industrial production growth, and one-year risk-free rate); and (iv) the sum of long-term innovations (long-run inflation and real rate trends), labeled Σ_{LR}. The error variance decompositions refer to horizons of 12 months (first row of each maturity) and 120 months (second row of each maturity).

4.3 Historical decomposition of four episodes.

In this section, we decompose the 2-year and 10-year US (EA) ILS rates and their expected and IRP components, respectively, around four historical episodes: (i) the GFC, which is characterized by an initial drop in ILS rates during the second half of 2008 – brought about by lower inflation expectations linked to the global slowdown caused by the crisis – and then by a rebound in the first half of the subsequent year; (ii) the oil price glut period, roughly spanning from mid-2014 to the end of 2015, and that is distinguished by downward pressure on inflation expectations; (iii) the COVID-19 era, ranging from early 2020 until the end of 2021. The period is marked by a sharp decline in ILS rates followed by an increasing trend that continued until the end of the period; and (iv) the Russian invasion in Ukraine, spanning throughout 2022, whereby ILS rates initially surged to historically high values, see Figure 1.

The second column of Panel A1 (A2) of Table 3 reports the changes in the 2-year

ILS during the periods indicated in the first column. These date ranges mark the most pronounced movements in ILS rates during these episodes. The subsequent column decomposes the ILS changes in (i) the sum of PC innovations (column 3), (ii) the contribution of international innovations (columns 4 to 5), (iii) the part related to local economic innovations (columns 6 to 8), and (iv) the long-run innovations (columns 9 to 10). Panels B and C are structured similarly but refer to the EC and IRP parts of the ILS changes, respectively. Table 4 repeats the analysis for the 10-year maturity.

Great Financial crisis.
Focusing on the 2-year contract during the GFC, Table 3 indicates that, in both regions, innovations to international factors, and in particular oil prices, played a key role in the stochastic movements of the ILS rates and its EC and IRP components. From June 2008 to December 2008, the US ILS rates experienced a drop of 563 bps, which is split between a 35% decrease in the EC (-198 bps) and a 65% decline in the IRP (-366 bps). The decrease in oil prices accounted for about 30% of the ILS rate drop, i.e., -175 bps. The other major factors pushing down those rates were the drop in inflation that is not accounted for by other factors (-123 bps), global (commodity) demand (-66 bps), and industrial production (-60 bps). The decomposition of ILS rates reveals that, while international innovations work mostly via the IRP channel – 78% of their total contribution relates to this channel – local macroeconomic factors evenly affected both the EC and the IRP. In the following months, from January 2009 to December 2009, ILS rates bounced back by 316 bps, and the relative contribution of individual innovations nearly mirrored the previous period but with a switch in sign. Oil price increases were the leading drivers of ILS and IRP surges (by 134 and 81 bps, respectively), followed by other transitory economic factors, particularly global demand and inflation. Over the same period, the 2-year EA ILS rates exhibit half of the variation compared to their US counterparts, with most of this volatility attributable to IRP movements. As in the US, oil price innovations were (one of) the dominant factors, accounting for 33% of the initial ILS drop and 46% of their subsequent increase. In contrast to the US case, our model indicates the importance of interest rates in explaining ILS movements in the EA. Interest rates were brought to very low levels at the end of the period and accounted for 38% of the drop in ILS rates. Monetary policy weighed on inflation compensation by accounting for more than 46% of the decline of IRP in the aftermath of Lehman's collapse.

Oil price glut.
During the oil price glut episodes of the mid-2010s, in both areas, the 2-year ILS rates oscillated over three consecutive periods, each time by about 100 basis points in absolute value. During the first phase of the oil glut, from June 2014 to December 2014, oil price innovations drove these fluctuations, accounting – mainly via the IRP channel – for more than 80% (90%) of the decrease in US (EA) ILS rates. In the second phase of the glut, the increase in oil prices contributed to the surge of ILS rates, mainly due to an increase in both the EC and IRP. Finally, during the last decline in oil prices, the drop in ILS was also linked to PC innovations, i.e., to factors not captured by our model.

Table 3: Detailed historical decomposition: 2-year ILS

US

Panel A1: Level

GFC	y_2	PCs	g^w	p^o	π	g	i	π^*	r^*
2008.06 2008.12	-563	-144	-66	-175	-123	-60	-14	5	14
2008.11 2009.06	316	63	40	134	57	-4	6	1	18
Oil Glut	y_2	PCs	g^w	p^o	π	g	i	π^*	r^*
2014.06 2014.12	-148	-18	2	-124	1	-4	2	4	-10
2014.12 2015.04	105	24	-5	94	9	-1	-9	1	-9
2015.04 2015.09	-92	-40	5	-36	-1	-11	-3	-2	-4
COVID-19	y_2	PCs	g^w	p^o	π	g	i	π^*	r^*
2019.12 2020.03	-208	2	-18	-183	10	0	-21	-2	4
2020.03 2020.08	218	-9	20	183	4	12	-3	-1	13
2020.10 2021.05	168	72	19	68	25	-12	-1	-3	0
2021.08 2021.11	67	71	-10	-30	40	-10	1	6	-1
Ukraine war	y_2	PCs	g^w	p^o	π	g	i	π^*	r^*
2021.12 2022.04	118	62	-1	42	-33	11	35	11	-9
2022.04 2022.09	-211	-125	-17	-82	-8	-14	38	15	-19

Panel B1: EC

GFC	y_2^{EC}	PCs	g^w	p^o	π	g	i	π^*	r^*
2008.06 2008.12	-198	-65	-23	-29	-57	-35	-12	12	12
2008.11 2009.06	143	28	21	54	32	4	8	-11	7
Oil Glut	y_2^{EC}	PCs	g^w	p^o	π	g	i	π^*	r^*
2014.06 2014.12	-26	-9	3	-21	1	3	2	8	-13
2014.12 2015.04	20	14	0	40	2	-14	-8	-4	-8
2015.04 2015.09	-19	-19	6	-2	3	0	-2	-3	-1
COVID-19	y_2^{EC}	PCs	g^w	p^o	π	g	i	π^*	r^*
2019.12 2020.03	-54	0	-5	-39	3	3	-20	0	2
2020.03 2020.08	94	-5	8	63	2	19	-1	-3	12
2020.10 2021.05	44	34	1	2	13	-7	-1	6	-3
2021.08 2021.11	48	33	-9	-11	21	7	1	8	-2
Ukraine war	y_2^{EC}	PCs	g^w	p^o	π	g	i	π^*	r^*
2021.12 2022.04	33	32	-6	-1	-17	0	33	11	-20
2022.04 2022.09	-44	-58	-4	-25	3	-5	33	20	-8

Panel C1: IRP

GFC	y_2^{IRP}	PCs	g^w	p^o	π	g	i	π^*	r^*
2008.06 2008.12	-366	-79	-43	-146	-66	-25	-2	-6	2
2008.11 2009.06	173	35	19	81	25	-8	-2	12	11
Oil Glut	y_2^{IRP}	PCs	g^w	p^o	π	g	i	π^*	r^*
2014.06 2014.12	-122	-9	-1	-104	-1	-7	0	-4	3
2014.12 2015.04	85	10	-4	54	7	13	0	6	0
2015.04 2015.09	-73	-21	-1	-34	-3	-10	-1	1	-3
COVID-19	y_2^{IRP}	PCs	g^w	p^o	π	g	i	π^*	r^*
2019.12 2020.03	-154	2	-13	-145	7	-3	-1	-2	2
2020.03 2020.08	125	-4	12	120	2	-6	-2	3	0
2020.10 2021.05	124	39	18	67	12	-5	0	-9	4
2021.08 2021.11	18	38	-1	-19	19	-17	0	-3	1
Ukraine war	y_2^{IRP}	PCs	g^w	p^o	π	g	i	π^*	r^*
2021.12 2022.04	85	30	5	42	-16	11	2	0	11
2022.04 2023.01	-184	-69	-22	-53	-16	-11	8	-9	-12

EA

Panel A2: Level

GFC	y_2	PCs	g^w	p^o	π	g	i	π^*	r^*
2008.06 2008.11	-283	-62	-49	-92	1	21	-108	2	3
2008.11 2009.06	149	99	18	69	-56	14	-4	4	4
Oil Glut	y_2	PCs	g^w	p^o	π	g	i	π^*	r^*
2014.06 2015.01	-92	-17	-7	-90	29	-7	4	-4	-2
2015.01 2015.04	113	27	-2	78	26	-10	-3	-1	-1
2015.04 2015.08	-74	-25	7	-47	-9	-2	4	-2	-1
COVID-19	y_2	PCs	g^w	p^o	π	g	i	π^*	r^*
2019.12 2020.03	-133	-28	-11	-86	-10	-6	9	-2	1
2020.03 2020.08	104	51	20	67	-8	-11	-15	-1	0
2020.10 2021.03	136	-2	10	65	61	1	4	-2	-1
2021.04 2021.12	145	54	5	-15	104	3	-4	-1	0
Ukraine war	y_2	PCs	g^w	p^o	π	g	i	π^*	r^*
2021.12 2022.04	219	80	15	39	41	6	35	2	0
2022.08 2023.01	-276	-187	-4	-41	-53	-6	14	6	-5

Panel B2: EC

GFC	y_2^{EC}	PCs	g^w	p^o	π	g	i	π^*	r^*
2008.06 2008.11	-120	-27	-1	-72	-11	7	-32	14	1
2008.11 2009.06	13	25	-6	42	-53	-4	-1	6	3
Oil Glut	y_2^{EC}	PCs	g^w	p^o	π	g	i	π^*	r^*
2014.06 2015.01	-62	-2	-2	-76	28	-3	1	-7	-1
2015.01 2015.04	101	11	1	52	42	-2	-1	-2	0
2015.04 2015.08	-61	-13	-2	-36	-10	0	1	0	0
COVID-19	y_2^{EC}	PCs	g^w	p^o	π	g	i	π^*	r^*
2019.12 2020.03	-85	-4	3	-78	0	-4	3	-4	0
2020.03 2020.08	9	9	-2	46	-38	-4	-5	2	0
2020.10 2021.03	56	-17	2	52	23	2	1	-6	0
2021.04 2021.12	130	17	2	-3	116	-2	-1	2	0
Ukraine war	y_2^{EC}	PCs	g^w	p^o	π	g	i	π^*	r^*
2021.12 2022.04	123	38	5	35	13	8	10	14	0
2022.08 2023.01	-228	-140	0	-28	-78	0	5	16	-3

Panel C2: IRP

GFC	y_2^{IRP}	PCs	g^w	p^o	π	g	i	π^*	r^*
2008.06 2008.11	-164	-35	-48	-20	12	14	-76	-12	2
2008.11 2009.06	136	74	24	27	-3	18	-3	-2	1
Oil Glut	y_2^{IRP}	PCs	g^w	p^o	π	g	i	π^*	r^*
2014.06 2015.01	-29	-14	-5	-13	1	-4	3	4	-1
2015.01 2015.04	12	16	-3	26	-16	-9	-2	0	0
2015.04 2015.08	-13	-11	9	-11	1	-1	3	-2	0
COVID-19	y_2^{IRP}	PCs	g^w	p^o	π	g	i	π^*	r^*
2019.12 2020.03	-48	-24	-13	-8	-10	-2	6	2	0
2020.03 2020.08	95	42	22	21	30	-7	-10	-3	1
2020.10 2021.03	79	15	8	13	38	-1	3	4	-1
2021.04 2021.12	15	38	3	-12	-13	5	-3	-3	0
Ukraine war	y_2^{IRP}	PCs	g^w	p^o	π	g	i	π^*	r^*
2021.12 2022.04	97	43	10	4	29	-2	25	-12	0
2022.08 2023.01	-48	-47	-3	-13	25	-6	9	-10	-2

Notes: For a 2-year US (EA) ILS contract, the second column of panels A1 to C1 (A2 to C2) report the changes in the stochastic part of the ILS rate level (y_2), the EC (y_2^{EC}), and inflation risk premia (y_2^{IRP}), respectively. The first columns report the periods over which the changes are computed, while the third columns reports the total changes in the PCs. The remaining columns list the changes in the other variables, labeled following the notation of Section 2.2. We drop the time subscript to ease the notation.

Our results concur with other findings obtained using alternative models and data. For example, using US household survey data, Kilian and Zhou (2022) shows that oil (gasoline) price drops were the key driver of short-term (one-year) expectations in these two phases. This result largely aligns with our EC historical decomposition for the US. In addition, David Elliott and Roberts-Sklar (2015) find a statistically significant effect of

oil prices on both US and EA area short-term (3-year) ILS over the period January 2009 to July 2015 while Conflitti and Cristadoro (2018) document for the EA an increase in the correlation between oil price changes and 1-year ILS rates for the period July 2014 - January 2016. Finally, using zero coupon and year-on-year inflation options Galati et al. (2018) highlight that over January 2013 - December 2015, 2-year and 10-year (see infra) deflation risk became more sensible to oil price changes concerning previous periods.

COVID-19 pandemic.
During the first phase of COVID-19, US (EA) ILS rates initially dropped by 208 bps (133 bps) following the collapse of the global economy induced by the widespread restrictive sanitary measures. Subsequently, they rose by 218 bps (104 bps). The separation of these variations in EC and IRP components highlights that US ILS variations are chiefly linked to the latter channel, with the cumulative effects of global demand and, to a larger extent, oil price innovation accounting for virtually all the variation of the ILS rates (and its decomposition). In the EA, the initial drop of ILS rates was linked to both EC (64% of total variation) and IRP fluctuations, while their subsequent increase was related to the IRP channel. Innovations related to oil price changes were key drivers of EC and IRP changes, followed by global demand, inflation, and PCs innovations.

In both areas, the post-COVID-19 period, which ranges from late 2020 to late 2021, is characterized by two surges in ILS rates, reflecting the concerns linked to rising global demand coupled with supply chain disruptions and the rebound of energy prices. The first increase started in October 2020, when US (EA) rates climbed by 168 bps (136 bps), mainly due to an increase in the IRP, which represented roughly three-quarters (three-fifths) of the total variation. In the US, international innovations were still the primary source of variation in ILS rates, even if (i) their relative importance dropped to roughly 50% of the total variation and (ii) they spawned variation only in the IRP component. Kilian and Zhou (2022) show that, over the same period, the recovery of gasoline prices energy accounted for an increase in one-year inflation expectations of around 70 bps and were unimportant for the five-year horizon. Our results partly confirm this finding as for the EC of the 1-year contract, the impact of oil innovations is about 35 bps but quickly dies out for longer maturities, i.e., 2 and 10 years; see also Table 4. In the EA, the climb in ILS rates is mainly linked to local inflation dynamics and oil innovations. Interestingly, our model reveals that part of the inflation-induced increase was linked to a rise in the EC, potentially indicating that market participants believed in a short-term, temporary climb in inflation, chiefly linked to oil and inflation innovations.

The second increase in the US (EA) began in August (April) 2021 and was mainly associated with changes in the EC of ILS rates, especially in the EA. In this region, the surge in the ILS rate was associated with the expectation of higher inflation rates in the following years due to concerns related to the near-term outlook of inflation dynamics – the cumulated contribution of inflation innovations accounted for virtually all the variation in the EC.

Ukraine invasion.
The last episode we inspect covers the recent Russian invasion of Ukraine. Contrary to the previous episodes, we document that (i) EA rates show greater variability than the US peers and (ii) EA ILS changes are driven by fluctuations in the EC, while the reverse is true for the US, which fluctuated, mainly following variations in IRP. For the US, the detailed decomposition highlights that most fluctuations in ILS rates (and its

EC and IRP components) relate to PCs and oil innovations. The EA decomposition reveals that the initial surge in observed rates is linked – at various degrees – to the cumulative contribution of PCs, inflation, oil, and interest rates innovation. In contrast, the subsequent decrease in ILS rates is mainly related to PC innovations. Domestic and oil factors play a more important role, consistent with the EA being more exposed to this conflict.

The historical decomposition of the 10-year contract (Table 4) highlights the following points. First, in line with the analysis of Section 4.1 in both areas, the ILS rates are less volatile than their shorter-maturity counterparts. The larger swings in ILS rates occur in both regions during the GFC. The decline and the subsequent recovery of ILS rates were largely associated with transitory innovations, i.e., international – oil in particular – local inflation and demand (with the addition of interest rates for the EA). These changes were largely connected to risk repricing, signaling that the market did foresee only a marginal impact of those innovations on long-term expected inflation – in line with the relatively stable pattern, especially for the EA, of the stochastic trend inflation over the period, see Figure A1. The relatively stable pattern of the long-term EC partly contrasts the findings of Galati et al. (2011), who measure (daily) long-run inflation expectations as the one-year forward rate in nine years, cleaned for liquidity premium, and find that during the GFC, this measure of inflation expectations became more sensitive to news about inflation and other domestic macroeconomic variables.

Second, before mid-2021, the changes in ILS rates were mostly due to variations in the IRP channel, with the EC varying for a maximum of 19 bps. After this date, corresponding to the last three periods of Table 4, our model signals an increase in the volatility in long-term ILS-based inflation expectations, which substantially contributed to ILS rate fluctuations. Using average estimates of two dynamic term structure models and EA data, Neri et al. (2022) show that, after mid-2021, there has been an increase in both the inflation risk premium and genuine inflation expectations of the 5-year ILS rates in 5 years, corroborating our results. For the US, our model attributes this increase in volatility chiefly to innovations to the stochastic trend for inflation, which became more volatile in the last part of the sample, see Figure A1. Conversely, for the EA, the increase in volatility of the EC component of the 10-year rates is mainly linked to transitory inflation innovations and, for the last period, also to PC innovations and variations in the stochastic trend of inflation. That also explains the forceful reaction of central banks during the post-Covid recovery to avoid a de-anchoring of inflation expectations.

In summary, the historical decomposition reveals the importance of international factors in shaping the dynamics of these rates during specific periods. While similarities exist between the US and the EA, there are also key differences, such as the importance of local innovations in shaping the EA market. The analysis also highlights that for short-term maturities (2 years), economic innovations work through the EC and the IRP channels, pointing out that they are incorporated in marked-based inflation expectation measures, even when refined from risk compensation. For longer maturities, the variations in ILS rates are mostly related to the IRP channel, even if we observe that during the recent COVID-19 crisis, the EC channel is becoming more volatile, partly due to the contribution of economic innovations.

Table 4: Detailed historical decomposition: 10-year ILS

US

Panel A1: Level

GFC	y_{10}	PCs	g^w	p^o	π	g	i	π^*	r^*
2008.06 2008.12	-167	-16	-36	-68	-33	-22	-8	7	10
2008.11 2009.06	142	50	19	40	17	3	3	-2	12
Oil Glut	y_{10}	PCs	g^w	p^o	π	g	i	π^*	r^*
2014.06 2014.12	-66	-15	-1	-47	0	-3	1	6	-8
2014.12 2015.04	15	-4	-5	29	3	1	-4	1	-7
2015.04 2015.09	-44	-12	0	-18	-2	-5	-2	-4	-2
COVID-19	y_{10}	PCs	g^w	p^o	π	g	i	π^*	r^*
2019.12 2020.03	-86	3	-11	-70	2	0	-11	-2	2
2020.03 2020.08	92	9	9	63	1	3	-3	0	10
2020.10 2021.05	59	26	12	26	6	-6	0	-2	-2
2021.08 2021.11	18	20	-2	-11	9	-5	1	8	-1
Ukraine war	y_{10}	PCs	g^w	p^o	π	g	i	π^*	r^*
2021.12 2022.04	37	-3	3	18	-10	5	19	13	-8
2022.04 2023.01	-69	-58	-16	-23	-5	-6	30	32	-22

EA

Panel A2: Level

GFC	y_{10}	PCs	g^w	p^o	π	g	i	π^*	r^*
2008.06 2008.11	-136	-23	-28	-37	-2	19	-67	1	1
2008.11 2009.06	90	62	-1	31	-17	19	-11	4	4
Oil Glut	y_{10}	PCs	g^w	p^o	π	g	i	π^*	r^*
2014.06 2015.01	-53	-16	-6	-34	9	-4	3	-3	-1
2015.01 2015.04	33	12	-5	31	9	-10	-2	-1	0
2015.04 2015.08	-24	-6	1	-17	-1	-1	3	-2	-1
COVID-19	y_{10}	PCs	g^w	p^o	π	g	i	π^*	r^*
2019.12 2020.03	-64	-21	-10	-34	-2	-1	6	-1	0
2020.03 2020.08	47	39	5	29	-4	-11	-9	-2	0
2020.10 2021.03	65	20	2	26	17	0	3	-2	0
2021.04 2021.12	66	32	12	-8	29	5	-2	-2	0
Ukraine war	y_{10}	PCs	g^w	p^o	π	g	i	π^*	r^*
2021.12 2022.04	88	30	3	15	14	3	22	1	0
2022.08 2023.01	-26	-9	-3	-15	-16	-1	17	5	-4

Panel B1: EC

GFC	y_{10}^{EC}	PCs	g^w	p^o	π	g	i	π^*	r^*
2008.06 2008.12	-8	-13	4	4	-13	-7	-3	17	3
2008.11 2009.06	5	6	0	9	7	1	2	-21	1
Oil Glut	y_{10}^{EC}	PCs	g^w	p^o	π	g	i	π^*	r^*
2014.06 2014.12	11	-2	1	3	0	1	1	11	-4
2014.12 2015.04	-5	3	2	6	0	-3	-2	-8	-2
2015.04 2015.09	-5	-4	0	2	1	0	-1	-4	0
COVID-19	y_{10}^{EC}	PCs	g^w	p^o	π	g	i	π^*	r^*
2019.12 2020.03	3	0	2	2	1	1	-6	2	1
2020.03 2020.08	6	-1	-1	6	0	4	0	-5	4
2020.10 2021.05	12	7	-2	-5	3	-1	0	13	-1
2021.08 2021.11	21	7	-1	-1	5	2	0	11	-1
Ukraine war	y_{10}^{EC}	PCs	g^w	p^o	π	g	i	π^*	r^*
2021.12 2022.04	14	6	0	-3	-4	0	10	12	-7
2022.04 2023.01	38	-11	1	0	-1	-3	11	45	-4

Panel B2: EC

GFC	y_{10}^{EC}	PCs	g^w	p^o	π	g	i	π^*	r^*
2008.06 2008.11	-16	-6	-1	-14	-2	1	-7	13	0
2008.11 2009.06	7	5	-1	8	-11	-1	-1	5	1
Oil Glut	y_{10}^{EC}	PCs	g^w	p^o	π	g	i	π^*	r^*
2014.06 2015.01	-17	0	0	-15	6	0	0	-7	0
2015.01 2015.04	19	2	0	10	9	0	0	-2	0
2015.04 2015.08	-12	-3	0	-7	-2	0	0	0	0
COVID-19	y_{10}^{EC}	PCs	g^w	p^o	π	g	i	π^*	r^*
2019.12 2020.03	-19	-1	0	-15	0	-1	1	-4	0
2020.03 2020.08	3	1	0	9	-8	-1	-1	2	0
2020.1 2021.03	6	-4	0	10	5	0	0	-6	0
2021.04 2021.12	27	3	0	-1	24	0	0	2	0
Ukraine war	y_{10}^{EC}	PCs	g^w	p^o	π	g	i	π^*	r^*
2021.12 2022.04	35	8	1	7	3	1	2	14	0
2022.08 2023.01	-35	-29	0	-5	-16	0	1	15	-1

Panel C1: IRP

GFC	y_{10}^{IRP}	PCs	g^w	p^o	π	g	i	π^*	r^*
2008.06 2008.12	-159	-3	-40	-72	-20	-14	-5	-10	6
2008.11 2009.06	137	44	19	31	10	3	0	19	11
Oil Glut	y_{10}^{IRP}	PCs	g^w	p^o	π	g	i	π^*	r^*
2014.06 2014.12	-77	-13	-2	-50	0	-3	1	-5	-4
2014.12 2015.04	20	-7	-7	23	3	4	-2	9	-4
2015.04 2015.09	-39	-8	0	-21	-3	-5	-1	1	-2
COVID-19	y_{10}^{IRP}	PCs	g^w	p^o	π	g	i	π^*	r^*
2019.12 2020.03	-89	3	-13	-72	2	-1	-6	-4	2
2020.03 2020.08	86	10	10	58	1	-1	-3	5	6
2020.10 2021.05	46	19	14	31	3	-5	0	-15	-1
2021.08 2021.11	-3	13	-1	-10	5	-7	0	-3	-1
Ukraine war	y_{10}^{IRP}	PCs	g^w	p^o	π	g	i	π^*	r^*
2021.12 2022.04	22	-9	3	22	-6	5	9	1	-2
2022.04 2023.01	-107	-47	-17	-23	-4	-4	19	-13	-18

Panel C2:IRP

GFC	y_{10}^{IRP}	PCs	g^w	p^o	π	g	i	π^*	r^*
2008.06 2008.11	-121	-17	-27	-23	0	17	-60	-12	1
2008.11 2009.06	83	57	0	22	-7	20	-11	-2	3
Oil Glut	y_{10}^{IRP}	PCs	g^w	p^o	π	g	i	π^*	r^*
2014.06 2015.01	-36	-16	-6	-20	3	-4	3	4	-1
2015.01 2015.04	14	10	-5	21	0	-10	-1	0	0
2015.04 2015.08	-12	-3	1	-10	1	-1	3	-2	0
COVID-19	y_{10}^{IRP}	PCs	g^w	p^o	π	g	i	π^*	r^*
2019.12 2020.03	-44	-20	-11	-19	-2	0	5	2	0
2020.03 2020.08	45	37	5	20	3	-10	-8	-3	0
2020.1 2021.03	59	23	2	15	13	0	2	4	0
2021.04 2021.12	39	29	12	-7	5	5	-2	-4	0
Ukraine war	y_{10}^{IRP}	PCs	g^w	p^o	π	g	i	π^*	r^*
2021.12 2022.04	53	23	2	8	12	2	19	-13	0
2022.08 2023.01	9	20	-3	-10	0	-1	16	-10	-3

Notes: For a 10-year US (EA) ILS contract, the second column of panels A1 to C1 (A2 to C2) report the changes in the stochastic part of the ILS rate level (y_{10}), the EC (y_{10}^{EC}), and inflation risk premia (y_{10}^{IRP}), respectively. The first columns report the periods when the changes are computed, while the third columns report the total changes in the PCs. The remaining columns list the changes in the other variables, labeled following the notation of Section 2.2. We drop the time subscript to ease the notation.

5 Conclusions

Measuring inflation expectations is important for inflation-targeting central banks. Doing so allows them to monitor whether expectations are anchored to their inflation target and steer policy accordingly. One source of information on expectations is inflation-linked

swap rates, as quoted on financial markets. These series are available at a high frequency and reflect market activity. However, the series also contains a risk premium component, which implies that they are not a pure measure of inflation expectations.

Our paper proposes a new model to decompose financial market indicators of inflation compensation into genuine inflation expectations and risk premiums. We develop a no-arbitrage term structure model with stochastic endpoints, distinguishing short-term determinants of inflation risk premia from economically grounded long-run determinants, such as the equilibrium real interest rate and the inflation target.

We document two main findings. First, the decomposition of ILS rates in expected component (EC) and an inflation risk premium (IRP) underscores that the latter is an important driver of ILS rates' variation, especially for the EA during the lowflation period. Furthermore, by further decomposing these two components in a deterministic and stochastic part (see Giannone et al., 2019), we point out that the EA models based solely on spanned factors might generate an oscillating behavior in the deterministic part of the EC. This problematic feature is absent in our model with macroeconomic factors. Second, we underline the importance of those macroeconomic factors in explaining the stochastic evolution of ILS rates and their EC and IRP parts. For example, the variance and the historical decompositions highlight that innovations in unspanned factors account for more than 45 % of the low-frequency movements in IRP. As a result, they are a primary source of return variation in several historical episodes, like the 2010s oil price glut.

References

Aastveit, K. A., H. C. Bjørnland, and J. L. Cross (2023, 05). Inflation Expectations and the Pass-Through of Oil Prices. *The Review of Economics and Statistics 105*(3), 733–743.

Abrahams, M., T. Adrian, R. Crump, E. Moench, and R. Yu (2016). Decomposing real and nominal yield curves. *Journal of Monetary Economics 84*(C), 182–200.

Ang, A., G. Bekaert, and M. Wei (2008). The term structure of real rates and expected inflation. *Journal of Finance 63*(2), 797–849.

Ang, A. and M. Piazzesi (2003). A no-arbitrage vector autoregression of term structure dynamics with macroeconomic and latent variables. *Journal of Monetary Economics 50*(4), 745–787.

Bauer, M. D. and G. D. Rudebusch (2017, March). Resolving the spanning puzzle in macro-finance term structure models. *Review of Finance 21*(2), 511–553.

Bauer, M. D. and G. D. Rudebusch (2020, May). Interest rates under falling stars. *American Economic Review 110*(5), 1316–54.

Baumann, U., M. Darracq Pariès, T. Westermann, M. Riggi, E. Bobeica, A. Meyler, B. Böninghausen, F. Fritzer, R. Trezzi, and J. Jonckheere (2021, September). Inflation expectations and their role in Eurosystem forecasting. Occasional Paper Series 264, European Central Bank.

Berardi, A. and A. Plazzi (2018, 02). Inflation Risk Premia, Yield Volatility, and Macro Factors. *Journal of Financial Econometrics 17*(3), 397–431.

Breach, T., S. D'Amico, and A. Orphanides (2020). The term structure and inflation uncertainty. *Journal of Financial Economics 138*(2), 388–414.

Böninghausen, B., G. Kidd, and R. de Vincent-Humphreys (2018). Interpreting recent developments in market-based indicators of longer-term inflation expectations. *ECB Economic Bulletin* (6).

Camba-Mendez, G. and T. Werner (2017). The inflation risk premium in the post-Lehman period. Working Paper Series 2033, European Central Bank.

Campbell, J. Y. and L. Viceira (2001, March). Who should buy long-term bonds? *American Economic Review 91*(1), 99–127.

Carriero, A., S. Mouabbi, and E. Vangelista (2018). UK term structure decompositions at the zero lower bound. *Journal of Applied Econometrics 33*(5), 643–661.

Chernov, M. and P. Mueller (2012). The term structure of inflation expectations. *Journal of Financial Economics 106*(2), 367–394.

Christensen, J., J. Lopez, and G. Rudebusch (2010). Inflation expectations and risk premiums in an arbitrage-free model of nominal and real bond yields. *Journal of Money, Credit and Banking 42*(s1), 143–178.

Cieslak, A. and C. Pflueger (2023). Inflation and asset returns. *Annual Review of Financial Economics 15*(1), 433–448.

Conflitti, C. and R. Cristadoro (2018, January). Oil prices and inflation expectations. Questioni di Economia e Finanza (Occasional Papers) 423, Bank of Italy, Economic Research and International Relations Area.

David Elliott, Chris Jackson, M. R. and M. Roberts-Sklar (2015). Does oil drive financial market measures of inflation expectations? *Bank of England, Bank Underground, 20 October*.

Dewachter, H. and L. Iania (2011). An extended macro-finance model with financial factors. *Journal of Financial and Quantitative Analysis 46*(6), 1893?1916.

Dovern, J., U. Fritsche, and J. Slacalek (2012). Disagreement among forecasters in G7 countries. *The Review of Economics and Statistics 94*(4), 1081–1096.

Fan, J. and R. Li (2001). Variable selection via nonconcave penalized likelihood and its oracle properties. *Journal of the American Statistical Association 96*(456), 1348–1360.

Fisher, I. (1896). Appreciation and interest: A study of the influence of monetary appreciation and depreciation on the rate of interest with applications to the bimetallic controversy and the theory of interest. *Publications of the American Economic Association 11*(4), 331–442.

Fleckenstein, M., F. A. Longstaff, and H. Lustig (2017, 02). Deflation Risk. *The Review of Financial Studies 30*(8), 2719–2760.

Galati, G., Z. Gorgi, R. Moessner, and C. Zhou (2018). Deflation risk in the euro area and central bank credibility. *Economics Letters 167*, 124–126.

Galati, G., S. Poelhekke, and C. Zhou (2011, March). Did the Crisis Affect Inflation Expectations? *International Journal of Central Banking 7*(1), 167–207.

Giannone, D., M. Lenza, and G. E. Primiceri (2019). Priors for the long run. *Journal of the American Statistical Association 114*(526), 565–580.

Harvey, A. C. (1990). *Forecasting, Structural Time Series Models and the Kalman Filter*. Cambridge University Press.

Haubrich, J., G. Pennacchi, and P. Ritchken (2012). Inflation expectations, real rates, and risk premia: Evidence from inflation swaps. *Review of Financial Studies 25*(5), 1588–1629.

Holston, K., T. Laubach, and J. C. Williams (2017). Measuring the natural rate of interest: International trends and determinants. *Journal of International Economics 108*, S59–S75. 39th Annual NBER International Seminar on Macroeconomics.

Hördahl, P. and O. Tristani (2014, September). Inflation Risk Premia in the Euro Area and the United States. *International Journal of Central Banking 10*(3), 1–47.

Joslin, S., A. Le, and K. J. Singleton (2013, 08). JFEC Invited Paper: Gaussian Macro-Finance Term Structure Models with Lags. *Journal of Financial Econometrics 11*(4), 581–609.

Joslin, S., K. Singleton, and H. Zhu (2011). A New Perspective on Gaussian Dynamic Term Structure Models. *Review of Financial Studies 24*(3), 926–970.

Joyce, M. A., P. Lildholdt, and S. Sorensen (2010). Extracting inflation expectations and inflation risk premia from the term structure: A joint model of the UK nominal and real yield curves. *Journal of Banking and Finance 34*(2), 281–294.

Kilian, L. (2009, June). Not all oil price shocks are alike: Disentangling demand and supply shocks in the crude oil market. *American Economic Review 99*(3), 1053–69.

Kilian, L. and X. Zhou (2022). The impact of rising oil prices on U.S. inflation and inflation expectations in 2020–23. *Energy Economics 113*, 106228.

Kozicki, S. and P. Tinsley (2001). Shifting endpoints in the term structure of interest rates. *Journal of Monetary Economics 47*(3), 613–652.

Mouabbi, S., J.-P. Renne, and Tschopp (2023). The dynamic nature of macroeconomic risk. Mimeo.

Neri, S., G. Bulligan, S. Cecchetti, F. Corsello, A. Papetti, M. Riggi, C. Rondinelli, and A. Tagliabracci (2022, September). On the anchoring of inflation expectations in the euro area. Questioni di Economia e Finanza (Occasional Papers) 712, Bank of Italy, Economic Research and International Relations Area.

Stevens, A. and J. Wauters (2021, August). Is euro area lowflation here to stay? Insights from a time-varying parameter model with survey data. *Journal of Applied Econometrics 36*(5), 566–586.

Stoffer, D. S. and K. D. Wall (1991). Bootstrapping State-Space Models: Gaussian Maximum Likelihood Estimation and the Kalman Filter. *Journal of the American Statistical Association 86*(416), 1024–1033.

Tibshirani, R. (1996). Regression Shrinkage and Selection Via the Lasso. *Journal of the Royal Statistical Society: Series B (Methodological) 58*(1), 267–288.

A Appendix

A.1 Data codes

Table A1: Data

Variable	**Source (and *codes*)**
Price inflation	ECB (*ICP.M.U2.Y.X02200.3.INX*)
	FRED (*CPIAUCSL*)
Industrial Production Index	ECB (*STS.M.I8.Y.PROD.NS0020.4.000*)
	FRED (*INDPRO*)
Risk-free rates	FRED (*DTB1YR*)[11]
Real oil price	ECB (*FM.M.GB.EUR.4F.CY.EUCRBRDT.HSTA*, *ICP.M.U2.Y.000000.3.INX*)
	FRED (*OILPRICE*, *CPIAUCSL*)
Index of global real economic activity	Dallas Fed (*igrea*)

Note: ECB data for the euro area are retrieved from the ECB data portal at https://data.ecb.europa.eu/. Data for the US are taken from the FRED database at https://fred.stlouisfed.org/. The global measure of real economic activity is available at: https://www.dallasfed.org/research/igrea.

[11] Since the series is discontinued until June 2008, prior to that date, we use the one-year rate obtained from Liu and Wu (2021)

A.2 Regression evidence of unspanned macro variation and unspanned macro risk

In our modeling setting, we impose that three ILS principal components entirely explain the cross-section of ILS rates. Also, the global, country-specific, and long-term trends contain information about the future evolution of ILS rates above the information spanned by the principal components. This modeling choice overwhelmingly simplifies the estimation of the model, as the estimation of the risk factor dynamics, see equation (17), can be (partially) separated from the yield curve fitting, see equation (24). In this section, we provide regression evidence supporting our modeling choice. We follow sections 4.2 and 5.1 of Bauer and Rudebusch (2017) and report model-free regression evidence of unspanned macro variation and unspanned macro risk.

Table A2: Unspanned macro variation

	US: adjusted R^2							EA: adjusted R^2						
	p_t^o	g_t^w	π_t	g_t	i_t	π_t^*	r_t^*	p_t^o	g_t^w	π_t	g_t	i_t	π_t^*	r_t^*
Joint	0.59	0.36	0.47	0.08	0.24	0.60	0.04	0.51	0.51	0.41	-0.01	0.64	0.76	0.60
PC1	0.18	0.23	0.39	0.06	0.21	0.49	0.00	0.33	0.28	0.30	0.00	0.40	0.67	0.00
PC2	0.36	0.13	0.04	0.00	0.00	0.05	0.05	0.01	0.05	0.11	0.00	0.15	0.08	0.45
PC3	0.04	0.00	0.04	0.03	0.03	0.05	0.00	0.17	0.17	0.00	0.00	0.08	0.00	0.15

Notes: The first row reports the adjusted R^2 of regressing each international, country-specific, and stochastic trend measure on the first three principal components of the ILS rates. The last three rows report the adjusted R^2 of performing the regressions only with the first (second row), second (third row), or third (fourth row) principal component.

Investigating for unspanned macro variation is equivalent to asking: Do ILS principal components embed all the information in the global, country-specific, and long-term trends? In other words, can we write each of those variables as a perfect linear combination of the ILS principal components? Table A2 depicts the first the adjusted R^2 of regressing each international, country-specific, and stochastic trends measures on (i) all the first three principal components of the ILS rates (first row) and (ii) on each principal component separately (remaining rows). The stochastic trends are proxied by the (i) one-year ahead CE inflation expectation and (ii) the difference between the one-year risk-free rate and the one-year ahead CE inflation expectation. Focusing on the first row, for the US, except for the log of oil prices and inflation expectations, all the adjusted R^2 are below 50%. For the EA, ILS factors capture substantial variation of the risk-free rate and inflation expectations. For the other variables, the explanatory power is roughly equal to or smaller than 50%. The information contained in the level of the ILS rates links mostly to the one-year risk-free rate, inflation expectation, and inflation rate. This aligns with intuition, as all these variables are directly or indirectly linked to inflation.

We now turn to the model-free analysis related to unspanned macro risk. We analyze the ex-post excess returns of entering at, time t, an n-period ILS contract as the fixed leg counterpart and then closing this position after twelve months, at *t+12*, by taking the opposite position on an *n-12* contract. We label this quantity $\mathcal{R}^n_{t,t+12}$ and we write it, in annual terms, as:

$$\mathcal{R}^n_{t,t+12} = Y_{n,t} - \frac{n-12}{n} Y_{n-12,t+12} - \frac{12}{n}\pi_{\tau,\tau+12}, \tag{38}$$

where $Y_{n,t}$ and $Y_{n-12,t+12}$ are ILS rates, and $\pi_{\tau,\tau+1}$ is the floating payment related to the strategy, i.e., the one-year inflation between the τ and $\tau+1$, and $\tau < t$ accounts for the lagged indexation. The first column of Table A3 reports the adjusted R^2 of regressing $\mathcal{R}^n_{t,t+12}$ on the first three principal ILS components, $\mathbf{p}_t$. The remaining columns report the coefficients and the increase in adjusted R^2 by adding to $\mathbf{p}_t$ either (i) the level of the global variables, columns two to four, (iii) the local variables, columns five to eight, and (iv) two proxies for the stochastic trends, last three columns.[12]

Although PCs tend to better explain realized returns of longer maturities contracts for both regions, the explanatory power of the current shape of the ILS term structure is stronger for the EA than for the US. In the US, global variables help to explain ILS returns, especially for shorter-term contracts. Oil prices are at the origin of these results, with the oil coefficient significant at any confidence level. The explanatory power of global factors is less pronounced in the EA but tends to increase with maturity. Contrary to the US, both factors are equally responsible for the increase in adjusted R-squared. In both areas, the local variables exhibit explanatory power associated with short-term contracts. However, the origins of this explanatory power differ between the US and the EA. In the US, the explanatory power is connected to inflation, whereas in the EA, it is mostly tied to short-term interest rates. Finally, turning to stochastic trends, we report that they are mostly linked to returns on EA short-term contracts (via the inflation trend), while there is little explanatory power in the US market.[13]

Overall, mixed evidence exists for the predictive power of international, local, and stochastic trend variables for ILS returns.

[12] In all cases the global variables have been standardized to have zero mean and standard deviation of 1%. P-values are based on Newey–West standard errors with automatic lags selection.

[13] We also perform the predictive regressions by using the two-year moving average of our proxy for stochastic trends as explanatory variables. The explanatory power of stochastic trends, in particular the one linked to inflation, increases both for the EA and the US.

Table A3: Unspanned macro risk

US realized returns

	$\mathbf{p}_t$	Global variables			Local variables				Stochastic trends		
ILS	R^2_{adj}	p^o_t	g^w_t	ΔR^2_{adj}	π_t	g_t	i_t	ΔR^2_{adj}	π^*_t	r^*_t	ΔR^2_{adj}
1-year	0.04	1.24	-0.45	0.21	-1.81	-0.10	0.07	0.07	0.37	0.14	0.01
pval		0.00	0.10		0.00	0.48	0.67		0.22	0.43	
2-year	0.10	1.98	-0.27	0.21	-1.66	-0.20	0.13	0.03	0.47	0.20	0.01
pval		0.00	0.47		0.03	0.36	0.57		0.28	0.40	
10-year	0.20	3.33	-0.70	0.16	-2.17	-0.13	-0.03	0.00	-0.09	0.07	-0.01
pval		0.00	0.27		0.10	0.72	0.94		0.90	0.88	

EA realized returns

	$\mathbf{p}_t$	Global variables			Local variables				Stochastic trends		
ILS	R^2_{adj}	p^o_t	g^w_t	ΔR^2_{adj}	π_t	g_t	i_t	ΔR^2_{adj}	π^*_t	r^*_t	ΔR^2_{adj}
1-year	0.15	0.37	-0.56	0.08	-1.68	-0.02	0.39	0.11	1.23	0.40	0.11
pval		0.09	0.04		0.01	0.43	0.06		0.01	0.07	
2-year	0.19	0.85	-0.94	0.09	-1.78	-0.05	0.62	0.07	2.09	0.58	0.09
pval		0.02	0.06		0.04	0.33	0.06		0.02	0.07	
10-year	0.29	2.28	-1.75	0.14	-1.79	-0.04	-0.20	0.00	1.13	-0.22	0.00
pval		0.00	0.02		0.24	0.74	0.71		0.50	0.67	

Notes: The first column reports the adjusted R^2 of regressing one-year realized excess returns on the first three principal components of the ILS rates. The remaining columns report the coefficients and the increase in adjusted R^2 by adding to $\mathbf{p}_t$ either (i) the level of the global variables, columns two to four, (iii) the local variables, columns five to eight, and (iv) two proxies for the stochastic trends, last three columns. In all cases, the global variables have been standardized to have zero mean and standard deviation of 1%. P-values are based on Newey–West standard errors with automatic lags selection.

A.3 Estimation results

We obtained the error bands and t-statistics via bootstrapped standard errors. We use 500 draws, obtained via the bootstrap procedure for state space models of Stoffer and Wall (1991), adapted to account for missing observations.

A.3.1 Parameter estimates

Table A4: US parameter estimates

parameter	times	mode	tStat		times	mode	tStat	parameter	times	mode	tStat	parameter	times	mode	tStat	parameter	times	mode	tStat
σ^{g^w,g^w}	1	15.68	16.98	$\phi_1^{g^w,g^w}$	1	1.09	32.42	$\phi_2^{g^w,i}$	10^2	-0.10	-1.50	$\phi_3^{p^o,g^w}$	1	-0.08	-4.53	μ^{π}	10^2	0.04	0.75
σ^{g^w,p^o}	1	1.90	1.40	$\phi_1^{g^w,p^o}$	1	0.05	2.54	$\phi_2^{g^w,l}$	10^2	-0.45	-1.86	$\phi_3^{p^o,p^o}$	1	0.17	7.29	μ^{i}	10^2	0.13	1.45
$\sigma^{g^w,\pi}$	10^2	1.55	1.67	$\phi_1^{g^w,\pi}$	10^2	0.48	0.69	$\phi_2^{g^w,s}$	10^2	-0.29	-2.49	$\phi_3^{p^o,\pi}$	1	0.02	1.97	μ^{l}	10^2	-0.34	-5.85
$\sigma^{g^w,g}$	10^2	0.10	0.07	$\phi_1^{g^w,g}$	1	0.02	0.92	$\phi_2^{g^w,c}$	10^2	0.13	2.41	$\phi_3^{p^o,g}$	1	-0.03	-1.57	μ^{s}	10^2	0.65	8.58
$\sigma^{g^w,i}$	10^4	0.60	0.63	$\phi_1^{g^w,i}$	10^2	0.08	1.59	$\phi_2^{p^o,g^w}$	1	-0.07	-3.55	$\phi_3^{p^o,i}$	10^2	0.22	1.96	μ^{c}	10^2	0.12	2.72
$\sigma^{g^w,l}$	10^2	2.16	2.02	$\phi_1^{g^w,l}$	10^2	0.21	1.10	$\phi_2^{p^o,p^o}$	1	-0.19	-9.25	$\phi_3^{p^o,l}$	10^2	0.43	1.17	π_0^*	1	0.03	11.29
$\sigma^{g^w,s}$	10^2	0.69	0.72	$\phi_1^{g^w,s}$	10^2	0.20	2.20	$\phi_2^{p^o,\pi}$	1	-0.09	-4.01	$\phi_3^{p^o,s}$	10^2	-0.19	-0.95	r_0^*	1	0.03	3.33
$\sigma^{g^w,c}$	10^4	0.17	0.18	$\phi_1^{g^w,c}$	10^2	-0.08	-1.78	$\phi_2^{p^o,g}$	1	-0.06	-3.75	$\phi_3^{p^o,c}$	10^2	-0.06	-0.63	σ^{ip}	10^2	0.37	6.60
σ^{p^o,p^o}	1	8.95	8.29	$\phi_1^{p^o,g^w}$	1	0.13	5.48	$\phi_2^{p^o,i}$	10^2	0.10	0.63	$\phi_3^{\pi,\pi}$	1	0.21	8.29	$\sigma^{ce,ip}$	1	0.03	66.65
$\sigma^{p^o,\pi}$	1	3.27	3.88	$\phi_1^{p^o,p^o}$	1	0.99	38.67	$\phi_2^{p^o,l}$	1	-0.01	-2.18	$\phi_3^{\pi,g}$	1	0.03	1.58	$\sigma_{lr}^{ce,\pi}$	10^2	0.08	61.22
$\sigma^{p^o,g}$	10^2	0.73	0.52	$\phi_1^{p^o,\pi}$	1	0.07	4.01	$\phi_2^{p^o,s}$	10^2	0.32	1.31	$\phi_3^{\pi,i}$	10^2	0.86	2.56	$\sigma_{lr}^{ce,i}$	10^2	0.51	15.84
$\sigma^{p^o,i}$	10^2	2.23	2.31	$\phi_1^{p^o,g}$	1	0.12	4.93	$\phi_2^{p^o,c}$	10^2	-0.19	-1.68	$\phi_3^{\pi,l}$	10^2	-0.53	-0.54	$\sigma_{sr}^{ce,\pi}$	10^2	0.77	23.91
$\sigma^{p^o,l}$	10^2	5.53	5.49	$\phi_1^{p^o,i}$	10^2	-0.31	-2.82	$\phi_2^{\pi,\pi}$	1	-0.16	-4.18	$\phi_3^{\pi,s}$	10^2	-0.34	-0.62	$\sigma_{sr}^{spf,\pi}$	10^2	0.20	7.30
$\sigma^{p^o,s}$	10^2	-0.57	-0.58	$\phi_1^{p^o,l}$	10^2	0.27	0.73	$\phi_2^{\pi,g}$	1	0.02	0.92	$\phi_3^{\pi,c}$	10^2	0.20	0.68	$\sigma_{lr}^{spf,\pi}$	10^2	0.08	9.62
$\sigma^{p^o,c}$	10^2	1.52	1.63	$\phi_1^{p^o,s}$	10^4	-0.96	-0.05	$\phi_2^{\pi,i}$	1	-0.02	-3.35	$\phi_3^{g,\pi}$	10^2	0.76	0.65	$\sigma_{lr}^{ce,i}$	10^2	0.08	7.44
$\sigma^{\pi,\pi}$	1	9.06	12.30	$\phi_1^{p^o,c}$	10^2	0.30	2.81	$\phi_2^{\pi,l}$	1	-0.05	-3.56	$\phi_3^{g,g}$	1	0.18	5.22	$\sigma_{sr}^{r,hlw}$	10^2	0.44	22.29
$\sigma^{\pi,g}$	10^2	-1.46	-1.14	$\phi_1^{\pi,\pi}$	1	0.42	9.79	$\phi_2^{\pi,s}$	10^2	0.91	1.39	$\phi_3^{g,i}$	10^2	0.19	1.43	$\alpha^{r,hlw}$	1	0.01	9.90
$\sigma^{\pi,i}$	10^2	2.02	2.23	$\phi_1^{\pi,g}$	1	0.22	6.39	$\phi_2^{\pi,c}$	10^2	-0.53	-1.55	$\phi_3^{g,l}$	10^2	0.84	1.83	β^{ip}	1	4.89	15.30
$\sigma^{\pi,l}$	10^2	3.66	3.96	$\phi_1^{\pi,i}$	1	0.01	3.13	$\phi_2^{g,\pi}$	1	0.01	0.76	$\phi_3^{g,s}$	10^2	0.04	0.16	$\beta^{r,hlw}$	1	0.37	9.12
$\sigma^{\pi,s}$	10^2	-2.04	-2.05	$\phi_1^{\pi,l}$	1	0.06	4.85	$\phi_2^{g,g}$	1	0.04	0.99	$\phi_3^{g,c}$	10^2	0.01	0.11	$\alpha_{sr}^{ce,\pi}$	10^2	0.07	1.16
$\sigma^{\pi,c}$	10^2	2.26	2.37	$\phi_1^{\pi,s}$	10^2	-0.65	-1.02	$\phi_2^{g,i}$	10^2	-0.31	-1.63	$\phi_3^{i,\pi}$	1	-0.07	-3.07	$\alpha_{lr}^{ce,\pi}$	1	0.02	152.67
$\sigma^{g,g}$	1	6.32	8.16	$\phi_1^{\pi,c}$	10^2	-0.02	-0.06	$\phi_2^{g,l}$	1	0.01	1.81	$\phi_3^{i,g}$	1	-0.03	-1.50	$\alpha_{lr}^{ce,i}$	1	0.02	27.78
$\sigma^{g,i}$	10^4	0.25	0.29	$\phi_1^{g,\pi}$	1	-0.02	-0.80	$\phi_2^{g,s}$	10^2	0.15	0.53	$\phi_3^{i,i}$	1	-0.15	-5.67	$\beta_{sr}^{ce,i}$	1	1.00	370.71
$\sigma^{g,l}$	10^2	-1.17	-1.16	$\phi_1^{g,g}$	1	0.11	1.40	$\phi_2^{g,c}$	10^2	0.37	2.61	$\phi_3^{i,l}$	1	0.02	1.31	λ_1	1	1.00	18071.80
$\sigma^{g,s}$	10^2	-0.40	-0.47	$\phi_1^{g,i}$	10^2	0.18	1.09	$\phi_2^{i,\pi}$	1	0.02	1.07	$\phi_3^{i,s}$	10^2	0.37	0.27	λ_2	1	0.96	104.61
$\sigma^{g,c}$	10^2	0.71	0.81	$\phi_1^{g,l}$	1	0.01	2.44	$\phi_2^{i,g}$	1	-0.05	-2.36	$\phi_3^{i,c}$	1	0.02	1.74	λ_3	1	0.93	22.69
$\sigma^{i,i}$	10^2	11.61	11.26	$\phi_1^{g,s}$	10^2	-0.40	-1.50	$\phi_2^{i,i}$	1	0.16	11.10	$\phi_3^{l,l}$	1	0.81	27.96	ρ_0	1	0.09	5.94
$\sigma^{i,l}$	10^2	2.37	2.47	$\phi_1^{g,c}$	10^2	-0.10	-0.82	$\phi_2^{i,l}$	1	-0.03	-1.65	$\phi_1^{l,s}$	1	-0.03	-1.28				
$\sigma^{i,s}$	10^2	0.70	0.72	$\phi_1^{i,\pi}$	1	0.31	9.71	$\phi_2^{i,s}$	10^2	-0.11	-0.07	$\phi_1^{l,c}$	10^2	-0.94	-0.90				
$\sigma^{i,c}$	10^2	-0.89	-0.93	$\phi_1^{i,g}$	1	0.03	1.50	$\phi_2^{i,c}$	1	-0.01	-1.23	$\phi_1^{s,l}$	1	0.06	1.94				
$\sigma^{l,l}$	10^2	12.74	17.66	$\phi_1^{i,i}$	1	0.94	39.35	$\phi_2^{g^w,g^w}$	1	0.06	2.49	$\phi_1^{s,s}$	1	0.85	24.42				
$\sigma^{l,s}$	10^2	0.61	0.72	$\phi_1^{i,l}$	1	0.10	5.04	$\phi_3^{g^w,p^o}$	1	-0.01	-0.77	$\phi_1^{s,c}$	1	0.01	0.72				
$\sigma^{l,c}$	10^4	-0.34	-0.75	$\phi_1^{i,s}$	1	0.06	2.88	$\phi_3^{g^w,\pi}$	1	0.03	4.64	$\phi_1^{c,l}$	1	-0.09	-3.89				
$\sigma^{s,s}$	10^2	13.82	14.54	$\phi_1^{i,c}$	1	-0.02	-0.89	$\phi_3^{g^w,g}$	1	-0.02	-1.83	$\phi_1^{c,s}$	1	0.38	7.00				
$\sigma^{s,c}$	10^2	-3.52	-4.19	$\phi_2^{g^w,g^w}$	1	-0.22	-8.80	$\phi_3^{g^w,i}$	10^4	0.97	0.20	$\phi_1^{c,c}$	1	0.58	15.09				
$\sigma^{c,c}$	10^2	9.87	12.11	$\phi_2^{g^w,p^o}$	1	-0.03	-1.52	$\phi_3^{g^w,l}$	10^2	0.34	1.94								
σ^{π^*,π^*}	10^2	5.21	4.73	$\phi_2^{g^w,\pi}$	1	-0.03	-3.59	$\phi_3^{g^w,s}$	10^2	0.14	1.45								
σ^{r^*,r^*}	10^2	3.96	3.83	$\phi_2^{g^w,g}$	10^4	-0.24	0.00	$\phi_3^{g^w,c}$	10^2	-0.06	-1.29								

Notes: The parameter names (columns 1, 4, 8, 12, and 16, respectively) closely follow the notation of sections 2 and 3. Each parameter estimate (mode) should be multiplied by the factor listed under the accompanying "times" column.

Table A5: EA parameter estimates

parameter	times	mode	tStat	parameter	times	mode	tStat	parameter	times	mode	tStat	parameter	times	mode	tStat	parameter	times	mode	tStat
σ^{g^w,g^w}	1	0.23	16.94	$\phi_1^{g^w,g^w}$	1	1.10	47.67	$\phi_2^{g^w,i}$	10^2	-0.09	-1.50	$\phi_3^{p^o,g^w}$	1	-0.08	-4.36	μ^{π^*}	10^2	0.03	0.60
σ^{g^w,p^o}	10^2	0.86	1.64	$\phi_1^{g^w,p^o}$	1	0.04	2.83	$\phi_2^{g^w,l}$	10^2	-0.29	-1.29	$\phi_3^{p^o,p^o}$	1	0.11	5.75	μ^i	10^2	-0.05	-0.55
$\sigma^{g^w,\pi}$	10^2	0.69	3.05	$\phi_1^{g^w,\pi}$	10^2	-0.16	-0.32	$\phi_2^{g^w,s}$	10^2	-0.04	-0.52	$\phi_3^{p^o,\pi}$	1	0.04	4.39	μ^l	10^2	-0.23	-5.89
$\sigma^{g^w,g}$	10^2	-0.60	-0.94	$\phi_1^{g^w,g}$	1	0.03	1.22	$\phi_2^{g^w,c}$	10^2	0.06	1.40	$\phi_3^{p^o,g}$	10^2	-0.34	-0.20	μ^s	10^2	0.46	9.16
$\sigma^{g^w,i}$	10^2	0.03	1.13	$\phi_1^{g^w,i}$	10^2	0.06	1.61	$\phi_2^{p^o,g^w}$	1	-0.12	-6.07	$\phi_3^{p^o,i}$	10^2	0.13	1.26	μ^c	10^2	0.44	10.16
$\sigma^{g^w,l}$	10^2	0.12	1.70	$\phi_1^{g^w,l}$	10^2	0.11	0.65	$\phi_2^{p^o,p^o}$	1	-0.31	-15.47	$\phi_3^{p^o,l}$	10^2	0.43	1.11	π_0^*	1	0.02	20.13
$\sigma^{g^w,s}$	10^2	0.01	0.71	$\phi_1^{g^w,s}$	10^2	0.09	1.44	$\phi_2^{p^o,\pi}$	1	-0.05	-4.82	$\phi_3^{p^o,s}$	10^2	0.04	0.24	r_0^*	1	0.02	5.32
$\sigma^{g^w,c}$	10^2	-0.02	-1.51	$\phi_1^{g^w,c}$	10^2	-0.02	-0.62	$\phi_2^{p^o,g}$	1	-0.07	-4.30	$\phi_3^{p^o,c}$	10^2	0.07	0.80	σ^{ip}	10^2	0.37	12.98
σ^{p^o,p^o}	1	0.08	11.25	$\phi_1^{p^o,g^w}$	1	0.10	5.20	$\phi_2^{p^o,i}$	10^4	-0.40	-0.03	$\phi_3^{\pi,\pi}$	1	0.25	11.84	$\sigma^{ce,ip}$	1	0.03	69.90
$\sigma^{p^o,\pi}$	1	0.01	5.86	$\phi_1^{p^o,p^o}$	1	1.14	43.27	$\phi_2^{p^o,l}$	10^2	-0.67	-1.21	$\phi_3^{\pi,g}$	1	0.05	3.06	$\sigma^{ce,\pi}_{lr}$	10^2	0.08	81.83
$\sigma^{p^o,g}$	1	0.03	4.95	$\phi_1^{p^o,\pi}$	10^2	0.75	0.63	$\phi_2^{p^o,s}$	10^2	-0.45	-1.93	$\phi_3^{\pi,i}$	10^2	-0.10	-0.37	$\sigma^{ce,i}_{lr}$	10^2	0.79	61.00
$\sigma^{p^o,i}$	10^2	0.03	1.69	$\phi_1^{p^o,g}$	1	0.09	4.36	$\phi_2^{p^o,c}$	10^2	-0.10	-0.95	$\phi_3^{\pi,l}$	1	-0.02	-2.01	$\sigma^{ce,\pi}_{sr}$	10^2	0.68	30.46
$\sigma^{p^o,l}$	10^2	0.30	4.99	$\phi_1^{p^o,i}$	10^2	-0.10	-1.03	$\phi_2^{\pi,\pi}$	1	0.18	7.76	$\phi_3^{\pi,s}$	1	0.02	4.95	$\sigma^{spf,\pi}_{sr}$	10^2	0.18	12.81
$\sigma^{p^o,s}$	10^2	-0.05	-3.52	$\phi_1^{p^o,l}$	10^2	0.04	0.08	$\phi_2^{\pi,g}$	10^2	-0.40	-0.24	$\phi_3^{\pi,c}$	10^2	-0.29	-1.25	$\sigma^{spf,\pi}_{lr}$	10^2	0.08	329.65
$\sigma^{p^o,c}$	10^4	-0.52	-0.66	$\phi_1^{p^o,s}$	10^2	0.39	2.05	$\phi_2^{\pi,i}$	10^2	-0.10	-0.24	$\phi_3^{g,\pi}$	1	-0.02	-2.15	$\sigma^{ce,i}_{sr}$	10^2	0.08	11.46
$\sigma^{\pi,\pi}$	1	0.02	9.09	$\phi_1^{p^o,c}$	10^2	0.15	1.52	$\phi_2^{\pi,l}$	1	0.05	4.56	$\phi_3^{g,g}$	1	0.21	7.33	$\sigma^{r,hlw}$	10^2	0.31	15.47
$\sigma^{\pi,g}$	1	-0.01	-2.40	$\phi_1^{\pi,\pi}$	1	0.18	6.00	$\phi_2^{\pi,s}$	1	-0.02	-3.09	$\phi_3^{g,i}$	10^2	-0.01	-0.22	$\alpha^{r,hlw}$	10^2	0.81	8.53
$\sigma^{\pi,i}$	10^4	0.60	0.38	$\phi_1^{\pi,g}$	1	0.14	6.92	$\phi_2^{\pi,c}$	10^2	-0.08	-0.31	$\phi_3^{g,l}$	10^4	-0.36	-0.02	β^{ip}	1	4.98	37.32
$\sigma^{\pi,l}$	10^2	0.14	2.45	$\phi_1^{\pi,i}$	10^2	0.23	0.61	$\phi_2^{g,\pi}$	10^2	-0.71	-0.71	$\phi_3^{g,s}$	10^2	-0.19	-2.42	$\beta^{r,hlw}$	1	0.41	14.63
$\sigma^{\pi,s}$	10^2	-0.03	-1.45	$\phi_1^{\pi,l}$	1	0.08	5.96	$\phi_2^{g,g}$	1	0.05	1.70	$\phi_3^{g,c}$	10^2	0.05	1.25	$\alpha^{ce,\pi}_{sr}$	10^2	0.07	1.40
$\sigma^{\pi,c}$	10^4	0.82	0.88	$\phi_1^{\pi,s}$	1	-0.03	-5.62	$\phi_2^{g,i}$	10^2	-0.02	-0.30	$\phi_3^{i,\pi}$	1	-0.21	-10.71	$\alpha^{ce,\pi}_{lr}$	10^2	0.04	2.85
$\sigma^{g,g}$	1	0.14	10.07	$\phi_1^{\pi,c}$	10^2	0.76	2.72	$\phi_2^{g,l}$	10^2	-0.31	-1.28	$\phi_3^{i,g}$	1	-0.05	-3.09	$\alpha^{ce,i}_{lr}$	1	0.01	14.64
$\sigma^{g,i}$	10^2	0.04	2.26	$\phi_1^{g,\pi}$	10^2	0.55	0.49	$\phi_2^{g,s}$	10^2	-0.23	-2.27	$\phi_3^{i,i}$	10^2	-0.04	-0.02	$\beta^{ce,i}_{sr}$	1	1.01	400.57
$\sigma^{g,l}$	10^2	-0.04	-0.78	$\phi_1^{g,g}$	1	-0.10	-3.60	$\phi_2^{g,c}$	10^2	0.07	1.38	$\phi_3^{i,l}$	1	0.04	2.23	λ_1	1	1.00	1742.74
$\sigma^{g,s}$	10^4	-0.22	-0.12	$\phi_1^{g,i}$	10^4	0.85	0.12	$\phi_2^{i,\pi}$	1	-0.11	-5.51	$\phi_3^{i,s}$	10^2	-0.55	-0.48	λ_2	1	0.98	120.80
$\sigma^{g,c}$	10^4	-0.14	-0.15	$\phi_1^{g,l}$	10^2	-0.53	-2.06	$\phi_2^{i,g}$	1	-0.06	-3.90	$\phi_3^{i,c}$	10^2	-0.07	-0.06	λ_3	1	0.87	45.19
$\sigma^{i,i}$	10^2	0.18	10.74	$\phi_1^{g,s}$	10^2	-0.03	-0.32	$\phi_2^{i,i}$	1	-0.03	-2.33	$\phi_3^{l,l}$	1	0.80	36.44	ρ_0	1	0.03	3.57
$\sigma^{i,l}$	10^2	0.28	4.19	$\phi_1^{g,c}$	10^2	0.06	1.34	$\phi_2^{i,l}$	10^2	0.88	0.51	$\phi_1^{l,s}$	1	0.02	1.44				
$\sigma^{i,s}$	10^2	0.02	0.65	$\phi_1^{i,\pi}$	1	0.49	24.57	$\phi_2^{i,s}$	1	-0.05	-4.08	$\phi_1^{l,c}$	10^2	0.26	0.40				
$\sigma^{i,c}$	10^2	-0.02	-1.70	$\phi_1^{i,g}$	1	-0.13	-7.01	$\phi_2^{i,c}$	10^2	0.42	0.38	$\phi_1^{s,l}$	1	0.23	9.51				
$\sigma^{l,l}$	10^2	0.48	12.15	$\phi_1^{i,i}$	1	0.98	56.61	$\phi_2^{g^w,g^w}$	1	0.05	2.87	$\phi_1^{s,s}$	1	0.90	33.20				
$\sigma^{l,s}$	10^4	-0.93	-0.36	$\phi_1^{i,l}$	1	-0.06	-3.27	$\phi_3^{g^w,p^o}$	10^2	-0.96	-0.84	$\phi_1^{s,c}$	10^2	0.16	0.10				
$\sigma^{l,c}$	10^2	0.01	1.29	$\phi_1^{i,s}$	1	0.08	5.07	$\phi_3^{g^w,\pi}$	1	0.02	5.01	$\phi_1^{c,l}$	1	-0.07	-3.98				
$\sigma^{s,s}$	10^2	0.20	13.01	$\phi_1^{i,c}$	1	-0.01	-0.69	$\phi_3^{g^w,g}$	1	-0.03	-1.42	$\phi_1^{c,s}$	1	0.28	11.06				
$\sigma^{s,c}$	10^4	-0.92	-1.02	$\phi_2^{g^w,g^w}$	1	-0.22	-12.47	$\phi_3^{g^w,i}$	10^2	0.01	0.37	$\phi_1^{c,c}$	1	0.72	25.40				
$\sigma^{c,c}$	10^2	0.10	17.39	$\phi_2^{g^w,p^o}$	1	-0.02	-1.63	$\phi_3^{g^w,l}$	10^2	0.30	1.82								
σ^{π^*,π^*}	10^2	0.02	6.10	$\phi_2^{g^w,\pi}$	1	-0.02	-4.17	$\phi_3^{g^w,s}$	10^2	0.03	0.43								
σ^{r^*,r^*}	10^2	0.20	4.27	$\phi_2^{g^w,g}$	1	0.02	1.44	$\phi_3^{g^w,c}$	10^2	-0.09	-2.73								

Notes: The parameter names (columns 1, 4, 8, 12, and 16, respectively) closely follow the notation of sections 2 and 3. Each parameter estimate (mode) should be multiplied by the factor listed under the accompanying "times" column.

A.3.2 Stochastic trends and model fit

Figure A1: Long-run inflation and equilibrium real rate

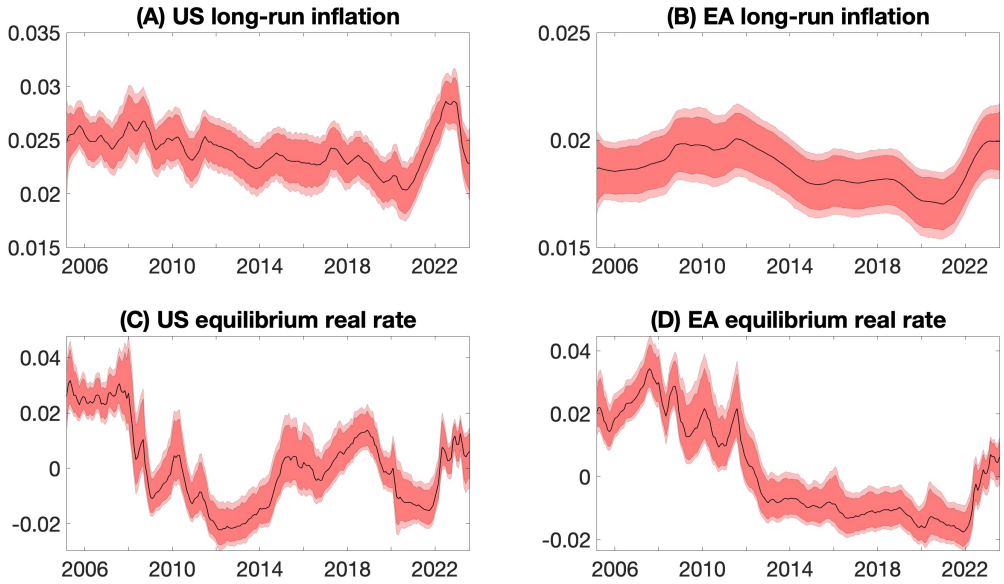

Notes: The top (bottom) panels report the long-run inflation (real rate) for the US and EA, left and right panels, respectively. The estimations refer to a model with three lags.

Figure A2: Fit of measurement equations

(a) Euro area

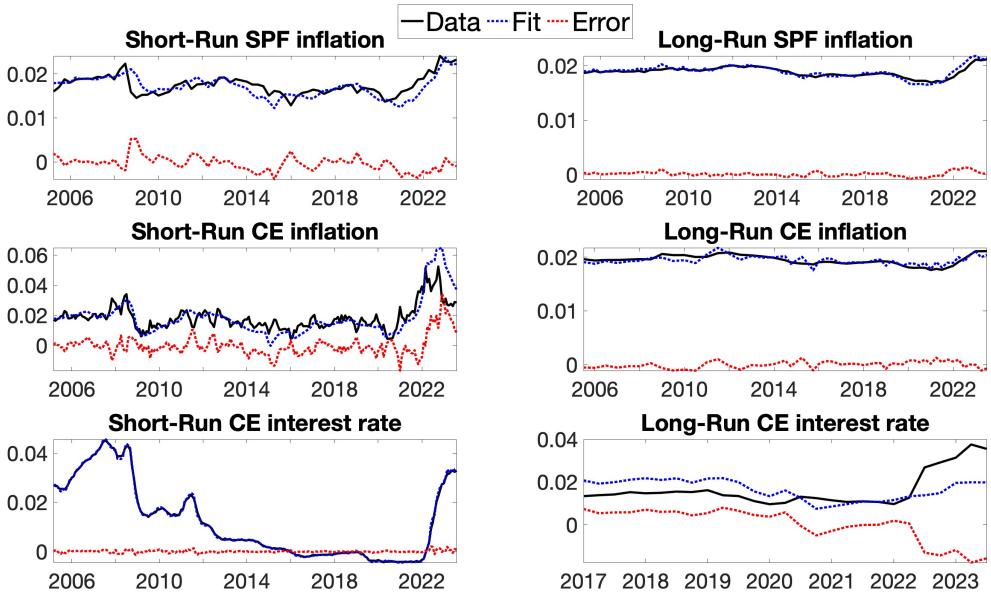

(b) United States

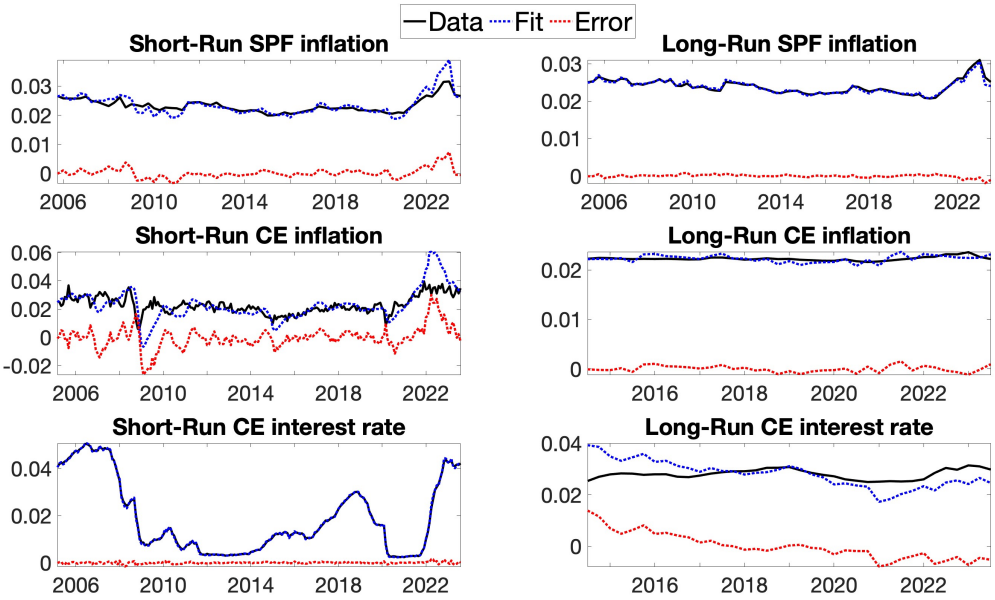

Notes: Model fit is shown for the EA and US in subfigures a and b, respectively. The top panels (A-C) concern, respectively, one-year-ahead Consensus Economics (CE) forecasts of industrial production, inflation, and the one-year risk-free rate. The middle panels concern the quarterly Survey of Professional Forecasters (SPF) forecasts of inflation (panels D and E) and the quarterly Holston et al. (2017) real-rate measure (panel F). The two bottom panels report the model fit for the quarterly long-term CE forecast of inflation (panel G) and the short-term rate (panel H). Each panel depicts the observed data in blue, with circled marks, and uses red lines for the filtered series from a six-lag model with international factors.

A.4 Additional tables

Table A6: EC and TP summary statistics

	2-year					10-year			
Full Sample	EA EC	EA TP	US EC	US TP	Full Sample	EA EC	EA TP	US EC	US TP
Min	0.0058	-0.0122	-0.0032	-0.0202	Min	0.0141	-0.0085	0.0157	-0.0059
Max	0.0455	0.0080	0.0311	0.0164	Max	0.0231	0.0090	0.0261	0.0119
Mean	0.0178	-0.0020	0.0173	0.0021	Mean	0.0172	0.0010	0.0183	0.0055
Std	0.0065	0.0041	0.0050	0.0055	Std	0.0016	0.0039	0.0018	0.0039
Autocorr	0.9358	0.8491	0.9515	0.8793	Autocorr	0.9540	0.9507	0.9417	0.9163
Pre Jan 2022	2-year				Pre Jan 2022	10-year			
Min	0.0058	-0.0122	-0.0032	-0.0202	Min	0.0141	-0.0085	0.0157	-0.0059
Max	0.0285	0.0061	0.0274	0.0164	Max	0.0194	0.0090	0.0213	0.0119
Mean	0.0163	-0.0024	0.0165	0.0018	Mean	0.0168	0.0007	0.0179	0.0057
Std	0.0037	0.0039	0.0043	0.0054	Std	0.0011	0.0038	0.0012	0.0039
Autocorr	0.8759	0.8705	0.9409	0.8741	Autocorr	0.9430	0.9543	0.9062	0.9231

Notes: For a 2-year US (EA) ILS contract panels A to D (E to H) report the error variance decomposition of the ILS rate level, the EC, inflation risk premia, and one year forward, respectively. Innovations are grouped as: (i) Σ_{PCs}, which is the sum of level, slope, and curvature innovations; (ii) Σ_{Gl}, namely the sum of oil and global real activity innovations; (iii) Σ_{Loc} representing the sum of the local macro variable innovations (month-on-month inflation, month-on-month industrial production growth, and one-year risk-free rate); and (iv) the sum of long-term innovations (long-run inflation and real rate trends), labeled Σ_{LR}. The error variance decompositions refer to horizons at three months (first row), 12 months (second row), 60 months (third row), and 120 months (fourth row).

A.5 Additional figures

Figure A3: 2-year and 10-year rates: deterministic components

(a) 2 years ILS contract: deterministic components

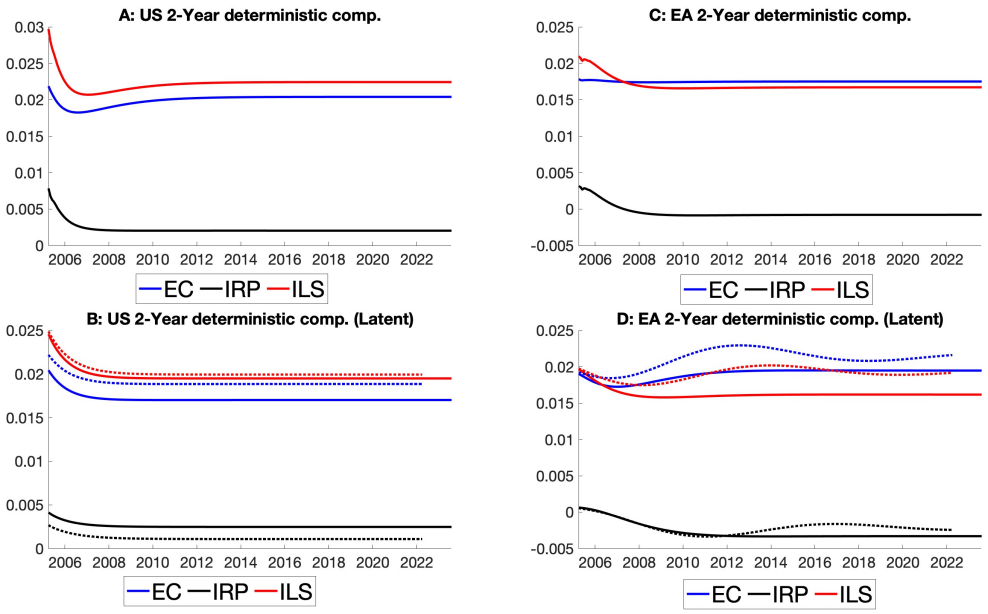

(b) 10 years ILS contract: deterministic components

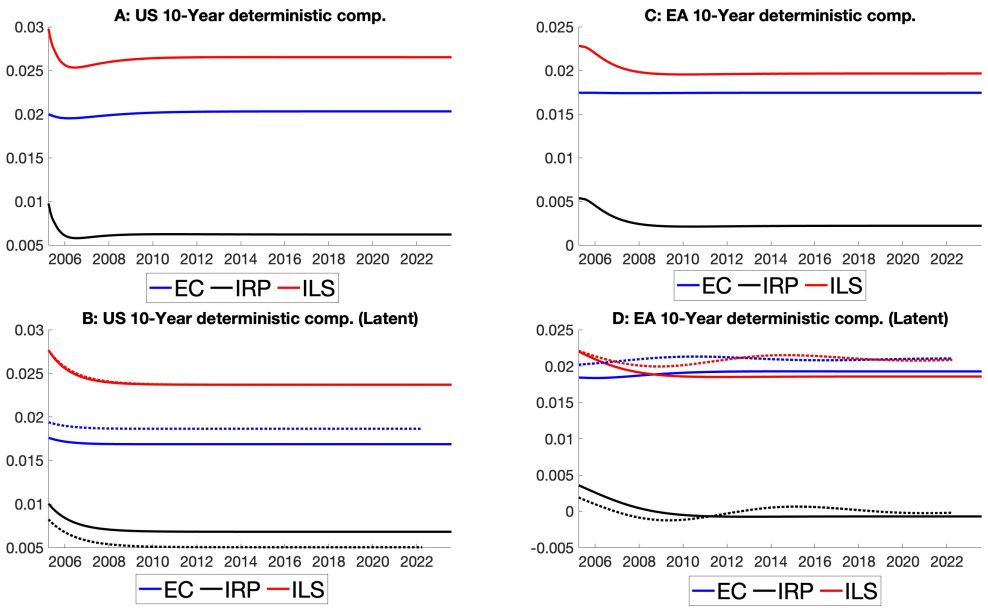

Notes: *Panel (a)*. For the 2-year ILS rates, the (sub) Panels of this figure report: (i) Panel A (E): the US (EA) ILS rates and their decompositions in EC and IRP; (ii) Panel B (F): the decomposition of the stochastic component of the US (EA) rates in EC and IRP; (iii) Panel C (G): the evolution of the deterministic component of the US (EA) rates and its decomposition in EC and IRP; (iv) Panel D (H): the evolution of the deterministic component of the US (EA) rates and its decomposition in EC and IRP for a model without unspanned risk factors and only Level, Slope, and Curvature. The dotted lines present the decomposition when estimating the latent model until March 2022. *Panel (b)* reproduces the same type of plots than *Panel (a)*, but for a 10-year ILS rates

NATIONAL BANK OF BELGIUM - WORKING PAPERS SERIES

The Working Papers are available on the website of the Bank: http://www.nbb.be.

405. “Robert Triffin, Japan and the quest for Asian Monetary Union”, I. Maes and I. Pasotti, *Research series*, February 2022.
406. “The impact of changes in dwelling characteristics and housing preferences on house price indices”, by P. Reusens, F. Vastmans and S. Damen, *Research series*, May 2022.
407. “Economic importance of the Belgian maritime and inland ports – Report 2020”, by I. Rubbrecht, *Research series*, May 2022.
408. “New facts on consumer price rigidity in the euro area”, by E. Gautier, C. Conflitti, R. P. Faber, B. Fabo, L. Fadejeva, V. Jouvanceau, J. O. Menz, T. Messner, P. Petroulas, P. Roldan-Blanco, F. Rumler, S. Santoro, E. Wieland and H. Zimmer, *Research series*, June 2022.
409. “Optimal deficit-spending in a liquidity trap with long-term government debt”, by Charles de Beauffort, *Research series*, July 2022.
410. “Losing prospective entitlement to unemployment benefits. Impact on educational attainment”, by B. Cockx, K. Declercq and M. Dejemeppe, *Research series*, July 2022.
411. “Integration policies and their effects on labour market outcomes and immigrant inflows”, by C. Piton and I. Ruyssen, *Research series*, September 2022.
412. “Foreign demand shocks to production networks: Firm responses and worker impacts”, by E. Dhyne, A. K. Kikkawa, T. Komatsu, M. Mogstad and F. Tintelnot, *Research series*, September 2022.
413. “Economic research at central banks: Are central banks interested in the history of economic thought?”, by I. Maes, *Research series*, September 2022.
414. “Softening the blow: Job retention schemes in the pandemic”, by J. Mohimont, M. de Sola Perea and M.-D. Zachary, *Research series*, September 2022.
415. “The consumption response to labour income changes, by K. Boudt, K. Schoors, M. van den Heuvel and J. Weytjens, *Research series*, October 2022.
416. “Heterogeneous household responses to energy price shocks, by G. Peersman and J. Wauters, *Research series*, October 2022.
417. “Income inequality in general equilibrium”, by B. Bernon, J. Konings and G. Magerman, *Research series*, October 2022.
418. “The long and short of financing government spending”, by J. Mankart, R. Priftis and R. Oikonomou, *Research series*, October 2022.
419. “Labour supply of households facing a risk of job loss”, by W. Gelade, M. Nautet and C. Piton, *Research series*, October 2022.
420. “Over-indebtedness and poverty: Patterns across household types and policy effects”, by S. Kuypers and G. Verbist, *Research series*, October 2022.
421. “Evaluating heterogeneous effects of housing-sector-specific macroprudential policy tools on Belgian house price growth”, by L. Coulier and S. De Schryder, *Research series*, October 2022.
422. “Bank competition and bargaining over refinancing”, by M. Emiris, F. Koulischer and Ch. Spaenjers, *Research series*, October 2022.
423. “Housing inequality and how fiscal policy shapes it: Evidence from Belgian real estate”, by G. Domènech-Arumì, P. E. Gobbi and G. Magerman, *Research series*, October 2022.
424. “Income inequality and the German export surplus”, by A. Rannenberg and Th. Theobald, *Research series*, October 2022.
425. “Does offshoring shape labor market imperfections? A comparative analysis of Belgian and Dutch firms”, by S. Dobbelaere, C. Fuss and M. Vancauteren, *Research series*, November 2022.
426. “Sourcing of services and total factor productivity”, E. Dhyne and C. Duprez, *Research series*, December 2022.
427. " Employment effect of citizenship acquisition: Evidence from the Belgian labour market", S. Bignandi and C. Piton, *Research series*, December 2022.
428. "Identifying Latent Heterogeneity in Productivity", R. Dewitte, C. Fuss and A. Theodorakopoulos, *Research series*, December 2022.
429. “Export Entry and Network Interactions - Evidence from the Belgian Production Network”, E. Dhyne, Ph. Ludwig and H. Vandenbussche, *Research series*, January 2023.
430. "Measuring the share of imports in final consumption", E. Dhyne, A.K. Kikkawa, M. Mogstad and F. Tintelnot, *Research series*, January 2023.
431. "From the 1931 sterling devaluation to the breakdown of Bretton Woods: Robert Triffin’s analysis of international monetary crises", I. Maes and I. Pasotti, *Research series*, January 2023.
432. “Poor and wealthy hand-to-mouth households in Belgium”, L. Cherchye, T. Demuynck, B. De Rock, M. Kovaleva, G. Minne, M. De Sola Perea and F. Vermeulen, *Research series*, February 2023.

433. “Empirical DSGE model evaluation with interest rate expectations measures and preferences over safe assets”, G. de Walque, Th. Lejeune and A. Rannenberg, *Research series*, February 2023.
434. “Endogenous Production Networks with Fixed Costs”, E. Dhyne, A. K. Kikkawa, X. Kong, M. Mogstad and F. Tintelnot, *Research series*, March 2023.
435. “BEMGIE: Belgian Economy in a Macro General and International Equilibrium model”, G. de Walque, Th. Lejeune, A. Rannenberg and R. Wouters, *Research series*, March 2023.
436. “Alexandre Lamfalussy and the origins of instability in capitalist economies”, I. Maes, *Research series*, March 2023.
437. “FDI and superstar spillovers: Evidence from firm-to-firm transactions”, M. Amiti, C. Duprez, J. Konings and J. Van Reenen, *Research series*, June 2023.
438. “Does pricing carbon mitigate climate change? Firm-level evidence from the European Union emissions trading scheme”, J. Colmer, R. Martin, M. Muûls and U.J. Wagner, *Research series*, June 2023.
439. “Managerial and financial barriers to the green transition”, R. De Haas, R. Martin, M. Muûls and H. Schweiger, *Research series*, June 2023.
440. “Review essay: The young Hayek”, I. Maes, *Document series*, September 2023.
441. “Review essay: Central banking in Italy”, I. Maes, *Document series*, September 2023.
442. “Debtor (non-)participation in sovereign debt relief: A real option approach”, D. Cassimon, D. Essers and A. Presbitero, *Research series*, September 2023.
443. “Input varieties and growth: a micro-to-macro analysis”, D.-R. Baqaee, A. Burstein, C. Duprez and E. Farhi, *Research series*, October 2023.
444. “The Belgian business-to-business transactions dataset 2002-2021”, E. Dhyne, C. Duprez and T. Komatsu, *Research series*, October 2023.
445. “Nowcasting GDP through the lens of economic states”, K. Boudt, A. De Block, G. Langenus and P. Reusens, *Research series*, December 2023.
446. “Macroeconomic drivers of inflation expectations and inflation risk premia”, J. Boeckx, L. Iania and J. Wauters, *Research series*, February 2024.

National Bank of Belgium
Limited liability company
Brussels RLP – Company's number: 0203.201.340
Registered office: 14 Boulevard de Berlaimont – BE-1000 Brussels
www.nbb.be

Editor

Pierre Wunsch
Governor of the National Bank of Belgium

Layout: Analysis and Research Group
Cover: NBB CM – Prepress & Image

Published in February 2024